

A General Decomposition Method for a Convex Problem Related to Total Variation Minimization

Stephan Hilb² and Andreas Langer^{1*}

^{1*}Department for Mathematical Sciences, Lund University,
Box 117, 221 00, Lund, Sweden.

²Stuttgart, Germany.

*Corresponding author(s). E-mail(s): andreas.langer@math.lth.se;

Abstract

We consider sequential and parallel decomposition methods for a dual problem of a general total variation minimization problem with applications in several image processing tasks, like image inpainting, estimation of optical flow and reconstruction of missing wavelet coefficients. The convergence of these methods to a solution of the global problem is analysed in a Hilbert space setting and a convergence rate is provided. Thereby, these convergence result hold not only for exact local minimization but also if the subproblems are just solved approximately. As a concrete example of an approximate local solution process a surrogate technique is presented and analysed. Further, the obtained convergence rate is compared with related results in the literature and shown to be in agreement with or even improve upon them. Numerical experiments are presented to support the theoretical findings and to show the performance of the proposed decomposition algorithms in image inpainting, optical flow estimation and wavelet inpainting tasks.

1 Introduction

The dimensionality of images has been tremendously increased in recent years due to the improvement of hardware. In order to further post-process

2 *A General Decomposition Method for a Convex Problem*

such large-scale data in a distributed parallel or memory-constrained setting, decomposition methods may be used, which split the original problem into a sequence of smaller subproblems that can be solved independently of each other while still approaching the original solution by means of an iterative algorithm. One particular approach are domain decomposition algorithms [8, 33, 34] which subdivide the problem domain. Typical examples of post-processing images include the removal of noise (denoising), the completion of missing data (inpainting) and the analysis of the data, as the computation of the optical flow in image sequences. In such applications one is usually interested in solutions in which edges are preserved. The total variation (TV) is well-know to promote discontinuities and hence is widely used in image processing tasks. Thereby one may consider the following regularized TV-model, cf. [14],

$$\inf_{u \in L^2(\Omega)^m \cap BV(\Omega)^m} \frac{1}{2} \|Tu - g\|_{L^2(\Omega)}^2 + \frac{\beta}{2} \|u\|_{L^2(\Omega)}^2 + \lambda \int_{\Omega} |Du|, \quad (1)$$

where $\Omega \subset \mathbb{R}^d$, $d \in \mathbb{N}$, is an open, bounded and simply connected domain with Lipschitz boundary, $g \in L^2(\Omega)$ describes the observed data, $T : L^2(\Omega)^m \rightarrow L^2(\Omega)$ with $m \in \mathbb{N}$ is a linear bounded operator, $\beta \geq 0$, $\lambda > 0$, and $\int_{\Omega} |Du|$ denotes the total variation of u in Ω defined by

$$\int_{\Omega} |Du| := \sup \left\{ \int_{\Omega} u \cdot \operatorname{div} \vec{v} \, dx : \vec{v} \in (C_0^{\infty}(\Omega))^{d \times m}, \right. \\ \left. |\vec{v}(x)|_F \leq 1 \text{ for almost every (f.a.e.) } x \in \Omega \right\}, \quad (2)$$

with $|\cdot|_F : \mathbb{R}^{d \times m} \mapsto \mathbb{R}$ being the Frobenius norm, cf. [13]. We recall that $BV(\Omega)^m$, i.e., the space of functions with bounded variation, equipped with the norm $\|\cdot\|_{BV} := \|\cdot\|_{L^1(\Omega)} + \operatorname{TV}(\cdot)$ is a Banach space [2, Theorem 10.1.1]. Note that $m \in \mathbb{N}$ describes the number of output channels, e.g., for grey-scale images we set $m = 1$ while for motion fields we have $m = d$.

The crucial difficulty of deriving decomposition methods for total variation minimization problems lies in the fact that the total variation is non-differentiable and non-additive with respect to a disjoint splitting of the domain Ω . In fact, let Ω_1 and Ω_2 be a disjoint decomposition of Ω , then we have the following splitting property, cf. [1, Theorem 3.84],

$$\int_{\Omega} |D(u|_{\Omega_1} + u|_{\Omega_2})| = \int_{\Omega_1} |D(u|_{\Omega_1})| + \int_{\Omega_2} |D(u|_{\Omega_2})| \\ + \int_{\partial\Omega_1 \cap \partial\Omega_2} |u|_{\Omega_1}^+ - u|_{\Omega_2}^-| \, d\mathcal{H}^{d-1}(x), \quad (3)$$

where \mathcal{H}^d denotes the Hausdorff measure of dimension d and the symbols u^+ and u^- the ‘‘interior’’ and ‘‘exterior’’ trace of u on $\partial\Omega_1 \cap \partial\Omega_2$ respectively. That is the total variation of a function of the whole domain equals the sum of the

total variation on the subdomains plus the size of the possible jumps at the interface. Exactly these jumps at the interfaces are important as we want to preserve crossing discontinuities and the correct matching where the solution is continuous. A failure of a decomposition method for total variation minimization has been reported in [9] with respect to a wavelet space decomposition. There a condition is derived which allows to check for global optimality of a limit point generated by the decomposition method. Although the method seems to work fine in practice, a counterexample showed in [9] that this condition does not hold in general. Nevertheless, this condition may be utilized in order to check a posteriori whether the splitting method found a good numerical approximation. First domain decomposition methods for total variation minimization are presented in [10, 11, 21]. Although their convergence and monotonic decay of the energy is theoretically ensured, the convergence to the solution of the global problem cannot be guaranteed in general, as counterexamples in [19, 22] illustrate. However, in [15, 16] an estimate of the distance of the numerical solution generated by such a decomposition method to the true minimizer of the original problem is derived. Utilizing this estimate demonstrated in [15, 16] that the splitting methods work in practice quite well for total variation minimization, as they indeed generate sequences for which this estimate indicates convergence to the global minimizer.

To overcome the difficulties due to the minimization of a non-smooth and non-additive objective in (1) a predual problem of (1), as in [7, 17] for the case $T = I$, $\beta = 0$, and $m = 1$, may be considered. In fact, a predual formulation of (1) can be derived which involves constrained minimization of a smooth functional [13].

Proposition 1.1 (cf. [13]). *Let $V := H_0^{\text{div}}(\Omega)^m$, $W := L^2(\Omega)^m$. Problem (1) is dual to*

$$\inf_{p \in K} \{ \mathcal{D}(p) := \frac{1}{2} \|\Lambda p - T^* g\|_{B^{-1}}^2 \}, \quad (4)$$

where $K := \{p \in V : |p(x)|_F \leq \lambda \text{ f.a.e. } x \in \Omega\}$, $\Lambda : V \rightarrow W$, $\Lambda p = \text{div } p$, $T^* : L^2(\Omega) \rightarrow W$ is the adjoint operators of T , $B : W \rightarrow W$ denotes the operator $B := \alpha_2 T^* T + \beta I$ and the norm is given by $\|u\|_{B^{-1}}^2 := \langle u, B^{-1} u \rangle_W$ for $u \in W$, where $\langle \cdot, \cdot \rangle_W$ denotes the W -inner product.

The unique solution \hat{u} of (1) is related to any solution \hat{p} of (4) by

$$\hat{u} = B^{-1}(-\Lambda \hat{p} + T^* g) \quad \text{and} \quad \forall p \in K : \langle \Lambda^* \hat{u}, p - \hat{p} \rangle_{V^*, V} \leq 0, \quad (5)$$

where $\Lambda^* : W^* \rightarrow V^*$ is the adjoint operators of Λ and $\langle \cdot, \cdot \rangle_{V^*, V}$ denotes the duality pairing between V and its dual space V^* .

Some comments on Proposition 1.1 are in order: To guarantee the existence of a minimizer of (4) we assume that the bilinear form $a_B : W \times W \rightarrow \mathbb{R}$, $a_B(u, v) := \alpha_2 \langle Tu, Tv \rangle_W + \beta \langle u, v \rangle_W$ is coercive [13, Theorem 3.5], i.e. $a_B(u, u) \geq c_B \|u\|_W^2$ with coercivity constant $c_B > 0$ and $\|\cdot\|_W$ being the norm induced by the W -inner product. In particular this implies the coercivity of

4 *A General Decomposition Method for a Convex Problem*

\mathcal{D} , i.e., for any feasible sequence $(p^n)_{n \in \mathbb{N}} \subset K$

$$\|p^n\|_V \rightarrow \infty \implies \mathcal{D}(p^n) \rightarrow \infty \quad (6)$$

with $\|\cdot\|_V$ being the norm associated to V [13]. Further the coercivity of a_B guarantees the invertibility of B [13]. Proposition 1.1 allows one to solve for \hat{p} in the predual domain of (4) and to later assemble the original solution \hat{u} using the optimality relation (5).

Here and in the sequel we write V and W instead of $H_0^{\text{div}}(\Omega)^m$ and $L^2(\Omega)^m$ as the below presented algorithms (see Algorithm 1 and Algorithm 2) as well as the associated theory also holds for problems of type (4) in a general Hilbert space setting, see Remark 6.6 below.

Based on a dualization as in Proposition 1.1 for the setting $T = I$, $\beta = 0$ and $m = 1$ in [7, 17] convergent overlapping and nonoverlapping domain decomposition methods are introduced. While the convergence in [17] for a nonoverlapping splitting is proven in a discrete setting, in [7] for an overlapping splitting even a convergence rate in a continuous setting is guaranteed. These two papers allowed to derive overlapping [20] and nonoverlapping [22] domain decomposition methods for the primal problem (1) in the respective setting and for $T = I$, $\beta = 0$ and $m = 1$, together with a convergence analysis which ensures that a minimizer of the global problem is indeed approached. Since then a series of splitting techniques for total variation minimization have been presented in the literature [23, 24, 25, 26, 28, 30, 31, 32]. For an introduction to domain decomposition approaches for total variation minimization we refer the reader to [19, 27].

In this paper we generalize the overlapping splitting method from [7], which is restricted to denoising, to the more general problem (4) where T can be any arbitrary linear and bounded operator, and hence to applications like inpainting and calculating the optical flow in image sequences. Further while the analysis of the decomposition method in [7] assumes exact local minimization, in our case an approximate local minimization is sufficient. This requires a new convergence analysis which differs significantly from the one in [7]. Moreover we are even able to improve the convergence rate of [7] by a constant. We provide a particular example in which the subproblems are approximated (solved inexactly) by so-called *surrogate* functionals, as in [10, 11, 16]. For solving the subproblems we adjust the semi-implicit algorithm by Chambolle [6] to our setting. While the algorithm in [6] is derived in a discrete setting and for image denoising problems only (i.e., $T = I$), we adjust it to our problem, where T might be any bounded and linear operator as already mentioned above, and Hilbert space setting.

We would like to mention that recently in [30] a general framework for analysing additive Schwarz methods of convex optimization problems as gradient methods has been presented. For the special case of parallel decomposition their analysis covers ours, while we extend our results to sequential decomposition which [30] does not cover. We also consider a slightly different notion of approximate minimization (see Definition 3.1) for the local subproblems

which does not seem to map to the approximate notion considered in [30] in an obvious way.

The rest of the paper is organized as follows: In Section 2 we introduce the setting of our decomposition which is based on the definition of a partition of unity operator. The proposed parallel and sequential decomposition algorithms are described in Section 3 and their convergence analysis is presented in Section 4. In particular we prove the convergence of the presented algorithms to a solution of the global problem together with a convergence rate. In Section 5 we compare our findings with related results already presented in the literature. As our proposed decomposition algorithms allow for approximate solutions of the subproblems, in Section 6 we present a concrete example for such a case utilizing the surrogate technique. For solving the constituted subdomain problems we describe in Section 7 the semi-implicit algorithm of Chambolle [6] in a general Hilbert space setting for our type of problems. In Section 8 numerical experiments are presented verifying the theoretical sublinear convergence of the proposed decomposition algorithms as well as showing the practical behaviour. We conclude in Section 9 with some final remarks.

2 Fundamentals

As we are presenting a decomposition method for (4) in the sequel we use the notations and definitions of Proposition 1.1. Further for a bounded linear operator $A : H_1 \rightarrow H_2$ between two Hilbert spaces H_1 and H_2 we use $\|A\|$ for the respective operator norm.

2.1 Decomposition Setting

We will analyse a decomposition algorithm for problem (4) that requires a suitable partition of unity respecting the closed convex set K or more precisely: bounded linear operators $\theta_i : V \rightarrow V$, $i = 1, \dots, M$, $M \in \mathbb{N}$ such that

$$I = \sum_{i=1}^M \theta_i \quad \text{and} \quad K = \sum_{i=1}^M \theta_i K. \quad (7)$$

Note here that, since θ_i is a bounded linear operator, $\theta_i K = \{\theta_i p : p \in K\} \subset V$ stays closed and convex.

The requirements for the partition given in (7) are in particular fulfilled by the following domain decomposition formulation. Let Ω_i , $i = 1, \dots, M$, $M \in \mathbb{N}$ be bounded open sets with Lipschitz boundary such that $\bigcup_{i=1}^M \Omega_i = \Omega$. Denote by $\tilde{\theta}_i : \Omega \rightarrow [0, 1]$, $i = 1, \dots, M$ a partition of unity satisfying

- (i) $\tilde{\theta}_i \in W^{1,\infty}(\Omega)$,
- (ii) $1 = \sum_{i=1}^M \tilde{\theta}_i$,
- (iii) $\text{supp } \tilde{\theta}_i \subset \bar{\Omega}_i$.

6 *A General Decomposition Method for a Convex Problem*

We then define the partition of unity operator $\theta_i : V \rightarrow V$ by pointwise multiplication

$$(\theta_i p)(x) := \tilde{\theta}_i(x)p(x), \quad (8)$$

for all $p \in V$.

Lemma 2.1. *The partition of unity operators $(\theta_i)_{i=1}^M$ defined in (8) satisfy the requirements of (7), where K is given by Proposition 1.1.*

Proof Linearity of θ_i , $i = 1, \dots, M$, is inherited from the pointwise multiplicative definition in (8). Let $p \in V = H_0^{\text{div}}(\Omega)^m$, then

$$\begin{aligned} \|\tilde{\theta}_i p\|_{L^2} &\leq \|\tilde{\theta}_i\|_{L^\infty} \|p\|_{L^2}, \\ \|\text{div}(\tilde{\theta}_i p)\|_{L^2} &= \|\nabla \tilde{\theta}_i p + \tilde{\theta}_i \text{div} p\|_{L^2} \\ &\leq \|\nabla \tilde{\theta}_i\|_{L^\infty} \|p\|_{L^2} + \|\tilde{\theta}_i\|_{L^\infty} \|\text{div} p\|_{L^2}, \end{aligned}$$

and thus, since $\tilde{\theta}_i \in W^{1,\infty}(\Omega)$ and in particular $\nabla \tilde{\theta}_i \in L^\infty(\Omega)$, we have proven that $\theta_i : V \rightarrow V$ is indeed well-defined and bounded.

Due to the pointwise nature of (8) we see that for $p \in V$:

$$\left(\sum_{i=1}^M \theta_i p \right)(x) = \sum_{i=1}^M \tilde{\theta}_i(x)p(x) = p(x)$$

which shows $I = \sum_{i=1}^M \theta_i$.

We have $K \subset \sum_{i=1}^M \theta_i K$ per definition. To show the other inclusion let $p^i \in \theta_i K$, $i = 1, \dots, M$. Then we see that in a pointwise fashion

$$\left| \sum_{i=1}^M p^i(x) \right|_F \leq \sum_{i=1}^M |p^i(x)|_F \leq \sum_{i=1}^M \tilde{\theta}_i(x) \lambda \leq \lambda,$$

thus showing that $p^i \in K$. □

3 Algorithm

Let us first introduce our notion of approximate minimization.

Definition 3.1. *For $q \in V$, $\rho \in (0, 1]$ we call*

$$\arg \min_{p \in K}^{\rho, q} \mathcal{D}(p) := \left\{ \tilde{p} \in K : \mathcal{D}(q) - \mathcal{D}(\tilde{p}) \geq \rho(\mathcal{D}(q) - \mathcal{D}(\hat{p})), \hat{p} \in \arg \min_{p \in K} \mathcal{D}(p) \right\} \quad (9)$$

the set of ρ -approximate minimizers of \mathcal{D} on K with respect to q .

The condition in (9) means that the improvement in functional value needs to be at least within a constant factor of the remaining difference in functional value towards a true minimizer. For $\rho = 1$ and arbitrary $q \in V$ this reduces to the usual notion of minimizers.

We present the decomposition procedures in Algorithms 1 and 2.

Algorithm 1 Parallel decomposition

Require: $p^0 \in K$ and $\sigma \in (0, \frac{1}{M}]$, $\rho \in (0, 1]$

- 1: **for** $n = 0, 1, 2, \dots$ **do**
- 2: **for** $i = 1, \dots, M$ **do**
- 3: $\tilde{v}_i^n \in \arg \min_{v_i \in \theta_i K}^{\rho, \theta_i p^n} \mathcal{D}(p^n + (v_i - \theta_i p^n))$
- 4: **end for**
- 5: $p^{n+1} = p^n + \sum_{i=1}^M \sigma(\tilde{v}_i^n - \theta_i p^n)$
- 6: **end for**

Algorithm 2 Sequential decomposition

Require: $p^0 \in K$ and $\sigma \in (0, 1]$, $\rho \in (0, 1]$

- 1: **for** $n = 0, 1, 2, \dots$ **do**
- 2: $p_0^n = p^n$
- 3: **for** $i = 1, \dots, M$ **do**
- 4: $\tilde{v}_i^n \in \arg \min_{v_i \in \theta_i K}^{\rho, \theta_i p^n} \mathcal{D}(p_{i-1}^n + (v_i - \theta_i p^n))$
- 5: $p_i^n = p_{i-1}^n + \sigma(\tilde{v}_i^n - \theta_i p^n)$
- 6: **end for**
- 7: $p^{n+1} = p_M^n$
- 8: **end for**

To treat both algorithms in a similar way, we use the convention $p_{i-1}^n := p^n$ for Algorithm 1 independent of $i \in \{1, \dots, M\}$. Having defined $\tilde{v}_i^n \in \theta_i K$ for $i \in \{1, \dots, M\}$ we also set $\tilde{p}_i^n := p_{i-1}^n + (\tilde{v}_i^n - \theta_i p^n) \in K$.

We observe that in each step $n \in \mathbb{N}_0$, $i \in \{1, \dots, M\}$ of Algorithms 1 and 2 the subproblem

$$\inf_{v_i \in \theta_i K} \frac{1}{2} \|\Lambda v_i - f_i^n\|_{B^{-1}}^2 \quad (10)$$

with $f_i^n = T^*g - \Lambda(p_{i-1}^n - \theta_i p^n)$ needs to be solved approximately.

For a locally acting operator B^{-1} and suitable θ_i these problems may be solved on $\text{supp}(\theta_i) \subset \bar{\Omega}$. If B^{-1} on the other hand is global then in order to avoid having to solve the subproblems globally on Ω a surrogate technique will be introduced in Section 6 below.

4 Convergence Analysis

In this section we analyse Algorithms 1 and 2 with respect to their convergence. In particular we first show monotonicity of the energy with respect to the iterates followed by the main results. Subsequently we collect useful statements which finally enable us to prove our main result at the end of this section.

4.1 Monotonicity

We first establish monotonicity of the iterates.

Lemma 4.1. *The iterates $(p^n)_{n \in \mathbb{N}}$ of Algorithms 1 and 2 with corresponding constraints on σ satisfy*

$$\mathcal{D}(p^n) - \mathcal{D}(p^{n+1}) \geq \rho\sigma \sum_{i=1}^M (\mathcal{D}(p_i^n) - \mathcal{D}(\hat{p}_i^n)) \geq 0$$

where $\hat{p}_i^n = p_{i-1}^n + (\hat{v}_i^n - \theta_i p^n)$, $\hat{v}_i^n \in \arg \min_{v_i \in \theta_i K} \mathcal{D}(p_{i-1}^n + (v_i - \theta_i p^n))$ denotes any exact minimizer in the i -th substep of the corresponding algorithm. The non-negative sequence $(\mathcal{D}(p^n))_{n \in \mathbb{N}}$ is in particular monotonically decreasing and thus convergent.

Proof The update step for p^{n+1} in the parallel case of Algorithm 1 is given as

$$p^{n+1} = p^n + \sigma \sum_{i=1}^M (\tilde{v}_i^n - \theta_i p^n) = (1 - \sigma M)p^n + \sigma \sum_{i=1}^M (p^n + (\tilde{v}_i^n - \theta_i p^n)).$$

We denote $\tilde{p}_i^n = p_{i-1}^n + (\tilde{v}_i^n - \theta_i p^n) = p^n + (\tilde{v}_i^n - \theta_i p^n)$. Since $\sigma \in (0, \frac{1}{M}]$, convexity of \mathcal{D} yields

$$\mathcal{D}(p^{n+1}) \leq (1 - \sigma M)\mathcal{D}(p^n) + \sigma \sum_{i=1}^M \mathcal{D}(\tilde{p}_i^n).$$

We use this and the definition of \tilde{v}_i^n to estimate

$$\begin{aligned} \mathcal{D}(p^n) - \mathcal{D}(p^{n+1}) &\geq \sigma M \mathcal{D}(p^n) - \sigma \sum_{i=1}^M \mathcal{D}(\tilde{p}_i^n) = \sigma \sum_{i=1}^M (\mathcal{D}(p^n) - \mathcal{D}(\tilde{p}_i^n)) \\ &\geq \rho\sigma \sum_{i=1}^M (\mathcal{D}(p^n) - \mathcal{D}(\hat{p}_i^n)), \end{aligned}$$

where we denoted $\hat{p}_i^n = p_{i-1}^n + (\hat{v}_i^n - \theta_i p^n) = p^n + (\hat{v}_i^n - \theta_i p^n)$ in the last inequality.

For the sequential case of Algorithm 2 we have similarly

$$\begin{aligned} p_i^n &= p_{i-1}^n + \sigma(\tilde{v}_i^n - \theta_i p^n) = (1 - \sigma)p_{i-1}^n + \sigma(p_{i-1}^n - (\tilde{v}_i^n - \theta_i p^n)) \\ &= (1 - \sigma)p_{i-1}^n + \sigma\tilde{p}_i^n \end{aligned}$$

and thus $\mathcal{D}(p_i^n) \leq (1 - \sigma)\mathcal{D}(p_{i-1}^n) + \sigma\mathcal{D}(\tilde{p}_i^n)$. Rewriting we see that

$$\mathcal{D}(p_{i-1}^n) - \mathcal{D}(p_i^n) \geq \sigma(\mathcal{D}(p_{i-1}^n) - \mathcal{D}(\tilde{p}_i^n)) \geq \rho\sigma(\mathcal{D}(p_{i-1}^n) - \mathcal{D}(\hat{p}_i^n)), \quad (11)$$

where we again used the definition of \tilde{v}_i^n in the second inequality. A telescope sum over $i = 1, \dots, M$ then yields

$$\mathcal{D}(p^n) - \mathcal{D}(p^{n+1}) = \sum_{i=1}^M (\mathcal{D}(p_{i-1}^n) - \mathcal{D}(p_i^n)) \geq \rho\sigma \sum_{i=1}^M (\mathcal{D}(p_{i-1}^n) - \mathcal{D}(\hat{p}_i^n)).$$

□

In particular, Lemma 4.1 shows monotonicity of energies, i.e. $\mathcal{D}(p^n) \geq \mathcal{D}(p^{n+1})$. Because of the coercivity assumption (6), the set of iterates $\{p^n : n \in \mathbb{N}_0\} \subset V$ is therefore bounded. We thus denote for some fixed minimizer $\hat{p} \in K$ of \mathcal{D} the finite radius

$$R_{\hat{p}} := \sup\{\|p - \hat{p}\|_V : p \in K, \mathcal{D}(p) \leq \mathcal{D}(p^0)\} < \infty. \quad (12)$$

4.2 Main Results

Now we are able to state our main convergence result providing a convergence rate of the proposed algorithms to a minimizer of the original (global) problem.

Theorem 4.2. *Let $(p^n)_{n \in \mathbb{N}_0}$ be the iterates from either one of Algorithms 1 and 2 and let $\hat{p} \in K$ denote a minimizer of \mathcal{D} . Algorithms 1 and 2 converge in the sense that $\mathcal{D}(p^n) \rightarrow \mathcal{D}(\hat{p})$. More specifically,*

$$\mathcal{D}(p^n) - \mathcal{D}(\hat{p}) \leq \begin{cases} (1 - \frac{\rho\sigma}{2\alpha})^n (\mathcal{D}(p^0) - \mathcal{D}(\hat{p})) & \text{if } n \leq n_0 \\ \frac{2\Phi^2}{\rho\sigma} \alpha^2 (n - n_0 + 1)^{-1} & \text{if } n \geq n_0, \end{cases}$$

where $\alpha := 1 + M\sigma\sqrt{2 - \rho + 2\sqrt{1 - \rho}}$ for Algorithm 2 and $\alpha := 1$ for Algorithm 1, $\Phi := \sqrt{\|B^{-1}\|} \|\Lambda\| C_\theta R_{\hat{p}}$ with $C_\theta := \left(\sum_{i=1}^M \|\theta_i\|^2\right)^{\frac{1}{2}}$ and $n_0 := \min\{n \in \mathbb{N}_0 : \mathcal{D}(p^n) - \mathcal{D}(\hat{p}) < \Phi^2 \alpha\}$.

Proof The proof is deferred to Section 4.4. □

The difference in the predual energy can be related to the L^2 -error of the primal variable in the following way:

Proposition 4.3. *Let $\hat{p} \in V$ be a minimizer of (4) and $\hat{u} \in W$ be the minimizer of (1). Then for all $p \in V$ and $u := B^{-1}(-\Lambda p + T^*g)$ we have*

$$\frac{c_B}{2} \|u - \hat{u}\|_W^2 \leq \mathcal{D}(p) - \mathcal{D}(\hat{p}).$$

Proof Due to coercivity of a_B we have for $v \in W$

$$\begin{aligned} c_B \|B^{-1}v\|_W^2 &\leq a_B(B^{-1}v, B^{-1}v) = \langle (T^*T + \beta I)B^{-1}v, B^{-1}v \rangle_W \\ &= \langle v, B^{-1}v \rangle_W = \|v\|_{B^{-1}}^2. \end{aligned}$$

By expanding the quadratic functional \mathcal{D} at \hat{p} and using optimality of \hat{p} , i.e. $\langle \mathcal{D}'(\hat{p}), p - \hat{p} \rangle \geq 0$, we then see that

$$\begin{aligned} \mathcal{D}(p) - \mathcal{D}(\hat{p}) &= \langle \mathcal{D}'(\hat{p}), p - \hat{p} \rangle_V + \frac{1}{2} \langle \Lambda^* B^{-1} \Lambda (p - \hat{p}), p - \hat{p} \rangle_V \\ &\geq \frac{1}{2} \|\Lambda(p - \hat{p})\|_{B^{-1}}^2 \geq \frac{c_B}{2} \|B^{-1} \Lambda(p - \hat{p})\|_W^2 = \frac{c_B}{2} \|u - \hat{u}\|_W^2, \end{aligned}$$

since due to Proposition 1.1 \hat{u} is given by $\hat{u} = B^{-1}(-\Lambda\hat{p} + T^*g)$. □

4.3 Collection of Useful Results

Here we collect some statements which we use to proof Theorem 4.2.

Definition 4.4. *For $p, q \in V$ we introduce the notation*

$$\langle p, q \rangle_* := \langle \Lambda^* B^{-1} \Lambda p, q \rangle_V, \quad \|p\|_* := \sqrt{\langle p, p \rangle_*}.$$

Note that we have $\|p\|_*^2 = \|\Lambda p\|_{B^{-1}}^2$ in particular and that $\langle \cdot, \cdot \rangle_*$ and $\|\cdot\|_*$ are not necessarily positive definite.

Lemma 4.5. *Let $\mathcal{D}' : V \rightarrow V$ be the Fréchet derivative of \mathcal{D} . For any $p, q, r \in V$ we have*

- (i) $\mathcal{D}(p) - \mathcal{D}(q) = \langle \mathcal{D}'(q), p - q \rangle_V + \frac{1}{2} \|p - q\|_*^2$,
- (ii) $\langle \mathcal{D}'(p) - \mathcal{D}'(q), r \rangle_V = \langle p - q, r \rangle_*$,

Proof (i) We expand the quadratic functional \mathcal{D} at q to obtain

$$\begin{aligned} \mathcal{D}(p) &= \mathcal{D}(q) + \langle \mathcal{D}'(q), p - q \rangle_V + \frac{1}{2} \langle \Lambda^* B^{-1} \Lambda(p - q), p - q \rangle_V \\ &= \mathcal{D}(q) + \langle \mathcal{D}'(q), p - q \rangle_V + \frac{1}{2} \|p - q\|_*^2 \end{aligned}$$

(ii) We see directly

$$\begin{aligned} \langle \mathcal{D}'(p) - \mathcal{D}'(q), r \rangle_V &= \langle \Lambda^* B^{-1} (\Lambda p - T^* g) - \Lambda^* B^{-1} (\Lambda q - T^* g), r \rangle_V \\ &= \langle \Lambda^* B^{-1} \Lambda(p - q), r \rangle_V = \langle p - q, r \rangle_*. \end{aligned}$$

□

We note that Lemma 4.5 actually holds true for any quadratic functional.

Lemma 4.6. *Let $c > 0$ and $(a_k)_{k \in \mathbb{N}_0} \subset \mathbb{R}^+$ be a sequence such that for all $k \in \mathbb{N}_0$:*

$$a_k - a_{k+1} \geq ca_k^2.$$

Then $\lim_{k \rightarrow \infty} a_k \rightarrow 0$ with rate

$$0 < a_k < \frac{1}{ck + \frac{1}{a_0}} < \frac{1}{ck}$$

for all $k \in \mathbb{N}$.

Proof We proceed similar to [5]. Since the iterates a_k , $k \in \mathbb{N}_0$ are monotonically decreasing, we can write for $k \in \mathbb{N}_0$:

$$\frac{1}{a_{k+1}} - \frac{1}{a_k} = \frac{a_k - a_{k+1}}{a_{k+1} a_k} \geq \frac{ca_k}{a_{k+1}} > c$$

and use it to reduce the telescope sum for $k > 0$:

$$\frac{1}{a_k} = \sum_{j=0}^{k-1} \left(\frac{1}{a_{j+1}} - \frac{1}{a_j} \right) + \frac{1}{a_0} > ck + \frac{1}{a_0}.$$

Inverting the inequality yields the statement. □

Lemma 4.7. *Let $a, b > 0$, $c, x, y \geq 0$ such that for all $\mu \in (0, 1]$ the inequality*

$$y \leq a\mu + \frac{b}{\mu}x + c\sqrt{x}$$

holds. Then the following split inequality holds:

$$y \leq \begin{cases} (2b + c\frac{\sqrt{b}}{\sqrt{a}})x & \text{if } x > \frac{a}{b}, \\ (2\sqrt{ab} + c)\sqrt{x} & \text{if } x \leq \frac{a}{b}, \end{cases} \quad (13)$$

or equivalently

$$x \geq \begin{cases} (2b + c\frac{\sqrt{b}}{\sqrt{a}})^{-1}y & \text{if } y > 2a + c\frac{\sqrt{a}}{\sqrt{b}}, \\ (2\sqrt{ab} + c)^{-2}y^2 & \text{if } y \leq 2a + c\frac{\sqrt{a}}{\sqrt{b}}. \end{cases}$$

Proof If $x > \frac{a}{b}$ we choose $\mu = 1$ to arrive at

$$y \leq a + bx + c\sqrt{x} < 2bx + c\sqrt{x} \leq (2b + c\frac{\sqrt{b}}{\sqrt{a}})x.$$

Otherwise we minimize the expression by choosing $\mu = \frac{\sqrt{b}}{\sqrt{a}}\sqrt{x}$ and get

$$y \leq a\frac{\sqrt{b}}{\sqrt{a}}\sqrt{x} + b\frac{\sqrt{a}}{\sqrt{b}}\sqrt{x} + c\sqrt{x} = (2\sqrt{ab} + c)\sqrt{x}.$$

Both statements together yield the estimate.

Noting that the right-hand side of estimate (13) is continuous and monotone in x , the case distinction can equivalently be written in terms of y by splitting at $x = \frac{a}{b}$, $y = (2b + c\frac{\sqrt{b}}{\sqrt{a}})\frac{a}{b} = 2a + c\sqrt{ab}$. Separately solving the inequalities for x thus yields the equivalent representation. \square

Lemma 4.8. *We have*

$$\sum_{i=1}^M \|\theta_i p\|_*^2 \leq \|B^{-1}\| \|\Lambda\|^2 C_\theta^2 \|p\|_V^2.$$

Proof Application of the Cauchy-Schwarz inequality yields

$$\begin{aligned} \sum_{i=1}^M \|\theta_i p\|_*^2 &= \sum_{i=1}^M \langle \Lambda \theta_i p, B^{-1} \Lambda \theta_i p \rangle_W \\ &\leq \sum_{i=1}^M \|B^{-1}\| \|\Lambda\|^2 \|\theta_i\|^2 \|p\|_V^2 = \|B^{-1}\| \|\Lambda\|^2 \left(\sum_{i=1}^M \|\theta_i\|^2 \right) \|p\|_V^2. \end{aligned}$$

\square

In the following we employ ideas from alternating minimization [5] to achieve a convergence rate estimate.

Lemma 4.9. *We may estimate the step distance in terms of the corresponding energy change as follows:*

$$\frac{1}{2} \|p_{i-1}^n - p_i^n\|_*^2 \leq \frac{\sigma}{\rho} (2 - \rho + 2\sqrt{1 - \rho}) (\mathcal{D}(p_{i-1}^n) - \mathcal{D}(p_i^n)).$$

Proof Let $\omega > 0$ to be chosen later and denote $\tilde{p}_i^n := p_{i-1}^n + (\tilde{v}_i^n - \theta_i p^n)$.

$$\begin{aligned}
\frac{1}{2\sigma^2} \|p_{i-1}^n - p_i^n\|_*^2 &= \frac{1}{2\sigma^2} \|\sigma(\tilde{v}_i^n - \theta_i p^n)\|_*^2 \\
&= \frac{1}{2} \|p_{i-1}^n - \tilde{p}_i^n\|_*^2 \\
&\leq \frac{1}{2} \left((1+\omega) \|p_{i-1}^n - \hat{p}_i^n\|_*^2 + (1+\omega^{-1}) \|\tilde{p}_i^n - \hat{p}_i^n\|_*^2 \right) \\
&\leq (1+\omega) (\mathcal{D}(p_{i-1}^n) - \mathcal{D}(\hat{p}_i^n)) + (1+\omega^{-1}) (\mathcal{D}(\tilde{p}_i^n) - \mathcal{D}(\hat{p}_i^n)) \\
&\hspace{10em} \text{(Lemma 4.5 (i) and optimality)} \\
&\leq \frac{1+\omega}{\rho} (\mathcal{D}(p_{i-1}^n) - \mathcal{D}(\tilde{p}_i^n)) + \frac{(1+\omega^{-1})(1-\rho)}{\rho} (\mathcal{D}(p_{i-1}^n) - \mathcal{D}(\tilde{p}_i^n)) \\
&\hspace{10em} \text{(due to (9))} \\
&= \frac{1}{\rho} (1+\omega + (1+\omega^{-1})(1-\rho)) (\mathcal{D}(p_{i-1}^n) - \mathcal{D}(\tilde{p}_i^n)) \\
&\leq \frac{1}{\sigma\rho} (1+\omega + (1+\omega^{-1})(1-\rho)) (\mathcal{D}(p_{i-1}^n) - \mathcal{D}(p_i^n)). \text{ (using (11))}
\end{aligned}$$

Choosing $\omega := \sqrt{1-\rho}$ so as to minimize the expression we arrive at

$$\frac{1}{2\sigma^2} \|p_{i-1}^n - p_i^n\|_*^2 \leq \frac{1}{\sigma\rho} (2-\rho + 2\sqrt{1-\rho}) (\mathcal{D}(p_{i-1}^n) - \mathcal{D}(p_i^n)).$$

□

Proposition 4.10. *Let $(p^n)_{n \in \mathbb{N}_0}$ be the iterates from either one of Algorithms 1 and 2 and let $\hat{p} \in K$ denote a minimizer of \mathcal{D} .*

Then $\mathcal{D}(p^n) \rightarrow \mathcal{D}(\hat{p})$ as $n \rightarrow \infty$ owing to

$$\mathcal{D}(p^n) - \mathcal{D}(\hat{p}) \leq \begin{cases} \frac{2}{\rho\sigma} \alpha (\mathcal{D}(p^n) - \mathcal{D}(p^{n+1})) & \text{if } \mathcal{D}(p^n) - \mathcal{D}(p^{n+1}) > \frac{1}{2} \sigma \rho \Phi^2, \\ \sqrt{\frac{2}{\rho\sigma}} \Phi \alpha \sqrt{\mathcal{D}(p^n) - \mathcal{D}(p^{n+1})} & \text{else,} \end{cases}$$

where $\alpha := 1 + M\sigma\sqrt{2-\rho+2\sqrt{1-\rho}}$ for Algorithm 2 and $\alpha := 1$ for Algorithm 1, and $\Phi := \sqrt{\|B^{-1}\| \|\Lambda\| C_\theta R_{\hat{p}}}$.

Proof Using convexity we expand

$$\begin{aligned}
\mathcal{D}(p^n) - \mathcal{D}(\hat{p}) &\leq \langle \mathcal{D}'(p^n), p^n - \hat{p} \rangle_V \\
&= \sum_{i=1}^M \langle \mathcal{D}'(p^n), \theta_i (p^n - \hat{p}) \rangle_V \\
&= \sum_{i=1}^M \left(\langle \mathcal{D}'(p_{i-1}^n), \theta_i (p^n - \hat{p}) \rangle_V + \sum_{j=1}^{i-1} \langle \mathcal{D}'(p_{j-1}^n) - \mathcal{D}'(p_j^n), \theta_i (p^n - \hat{p}) \rangle_V \right).
\end{aligned} \tag{14}$$

Let $\Phi_n := (\sum_{i=1}^M \|\theta_i(p^n - \hat{p})\|_*^2)^{\frac{1}{2}}$, $\hat{v}_i^n \in \arg \min_{v_i \in \theta_i K} \mathcal{D}(p_{i-1}^n + (v_i - \theta_i p^n))$ and $\tilde{p}_i^n := p_{i-1}^n + (\hat{v}_i^n - \theta_i p^n)$. We now estimate the first summand in the expansion above:

$$\begin{aligned}
&\sum_{i=1}^M \langle \mathcal{D}'(p_{i-1}^n), \theta_i (p^n - \hat{p}) \rangle_V \\
&= \frac{1}{\mu} \sum_{i=1}^M \langle \mathcal{D}'(p_{i-1}^n), \mu \theta_i (p^n - \hat{p}) \rangle_V
\end{aligned}$$

$$\begin{aligned}
&= \frac{\mu}{2} \sum_{i=1}^M \|\theta_i(p^n - \hat{p})\|_*^2 + \frac{1}{\mu} \sum_{i=1}^M (\mathcal{D}(p_{i-1}^n) - \mathcal{D}(p_{i-1}^n - \mu\theta_i(p^n - \hat{p}))) \\
&\quad \text{(Lemma 4.5 (i))} \\
&= \frac{\Phi_n^2 \mu}{2} + \frac{1}{\mu} \sum_{i=1}^M \left(\mathcal{D}(p_{i-1}^n) - \mathcal{D}(p_{i-1}^n + ((1-\mu)\theta_i p^n + \mu\theta_i \hat{p} - \theta_i p^n)) \right) \\
&\leq \frac{\Phi_n^2 \mu}{2} + \frac{1}{\mu} \sum_{i=1}^M (\mathcal{D}(p_{i-1}^n) - \mathcal{D}(\hat{p}_i^n)) \quad \text{(optimality)} \\
&\leq \frac{\Phi_n^2 \mu}{2} + \frac{1}{\mu\rho\sigma} (\mathcal{D}(p^n) - \mathcal{D}(p^{n+1})), \quad \text{(Lemma 4.1)}
\end{aligned}$$

where optimality was used by realizing that $(1-\mu)\theta_i p^n + \mu\theta_i \hat{p} \in \theta_i K$. For the second summand we see

$$\begin{aligned}
&\sum_{i=1}^M \sum_{j=1}^{i-1} \langle \mathcal{D}'(p_{j-1}^n) - \mathcal{D}'(p_j^n), \theta_i(p^n - \hat{p}) \rangle_V \\
&= \sum_{i=1}^M \sum_{j=1}^{i-1} \langle p_{j-1}^n - p_j^n, \theta_i(p^n - \hat{p}) \rangle_* \quad \text{(Lemma 4.5 (ii))} \\
&\leq \sum_{i=1}^M \sum_{j=1}^{i-1} \|p_{j-1}^n - p_j^n\|_* \|\theta_i(p^n - \hat{p})\|_* \\
&\leq M \left(\sum_{j=1}^M \|p_{j-1}^n - p_j^n\|_*^2 \right)^{\frac{1}{2}} \left(\sum_{i=1}^M \|\theta_i(p^n - \hat{p})\|_*^2 \right)^{\frac{1}{2}} \\
&\leq M\Phi_n \left(\sum_{j=1}^M \|p_{j-1}^n - p_j^n\|_*^2 \right)^{\frac{1}{2}}.
\end{aligned}$$

Applying Lemma 4.9 completes the estimate of the second summand, yielding

$$\begin{aligned}
&\sum_{i=1}^M \sum_{j=1}^{i-1} \langle \mathcal{D}'(p_{i-1}^n) - \mathcal{D}'(p_i^n), \theta_j(p^n - \hat{p}) \rangle_V \\
&\leq M\Phi_n \sqrt{\frac{2\sigma}{\rho} (2-\rho + 2\sqrt{1-\rho})} (\mathcal{D}(p^n) - \mathcal{D}(p^{n+1}))^{\frac{1}{2}}.
\end{aligned}$$

Combining both estimates and roughly bounding $\Phi_n \leq \Phi$ due to Lemma 4.8 we have

$$\begin{aligned}
\mathcal{D}(p^n) - \mathcal{D}(\hat{p}) &\leq \frac{\Phi^2 \mu}{2} + \frac{1}{\mu\rho\sigma} (\mathcal{D}(p^n) - \mathcal{D}(p^{n+1})) \\
&\quad + M\Phi \sqrt{\frac{2\sigma}{\rho} (2-\rho + 2\sqrt{1-\rho})} (\mathcal{D}(p^n) - \mathcal{D}(p^{n+1}))^{\frac{1}{2}}.
\end{aligned}$$

Invoking Lemma 4.7 with $a = \frac{\Phi^2}{2}$, $b = \frac{1}{\rho\sigma}$ and $c = M\Phi \sqrt{\frac{2\sigma}{\rho} (2-\rho + 2\sqrt{1-\rho})}$ yields the split bound with the following coefficients:

$$\begin{aligned}
2b + c\sqrt{\frac{b}{a}} &= \frac{2}{\rho\sigma} + M\Phi \sqrt{\frac{2\sigma}{\rho} (2-\rho + 2\sqrt{1-\rho})} \sqrt{\frac{2}{\sigma\rho\Phi^2}} \\
&= \frac{2}{\rho\sigma} (1 + M\sigma \sqrt{2-\rho + 2\sqrt{1-\rho}}),
\end{aligned}$$

$$\begin{aligned} 2\sqrt{ab} + c &= 2\sqrt{\frac{\Phi^2}{2\rho\sigma}} + M\Phi\sqrt{\frac{2\sigma}{\rho}(2-\rho+2\sqrt{1-\rho})} \\ &= \sqrt{\frac{2}{\rho\sigma}}\Phi(1 + M\sigma\sqrt{2-\rho+2\sqrt{1-\rho}}), \end{aligned}$$

which concludes the proof for Algorithm 2.

For Algorithm 1, examining the proof above, we notice that for the parallel version we have $p_i^n = p_{i-1}^n = p^n$ for $i = 1, \dots, M-1$ and thus the second summand in (14) vanishes completely. This allows us to invoke Lemma 4.7 with $c = 0$ and leads to the desired statement. \square

Now we are able to prove our main result.

4.4 Proof of Theorem 4.2

We first observe that since $(\mathcal{D}(p^n))_{n \in \mathbb{N}_0}$ is monotonically decreasing, n_0 is well-defined and we have $\mathcal{D}(p^n) - \mathcal{D}(\hat{p}) \geq \Phi^2\alpha$ for all $n \in \mathbb{N}_0$, $n < n_0$ and likewise $\mathcal{D}(p^n) - \mathcal{D}(\hat{p}) < \Phi^2\alpha$ for all $n \in \mathbb{N}_0$, $n \geq n_0$.

We now make use of Proposition 4.10. The equivalence in Lemma 4.7 then yields

$$\mathcal{D}(p^{n-1}) - \mathcal{D}(p^n) \geq \begin{cases} \frac{\rho\sigma}{2\alpha}(\mathcal{D}(p^{n-1}) - \mathcal{D}(\hat{p})) & \text{if } n-1 < n_0 \\ \frac{\rho\sigma}{2\Phi^2\alpha^2}(\mathcal{D}(p^{n-1}) - \mathcal{D}(\hat{p}))^2 & \text{if } n-1 \geq n_0. \end{cases}$$

In the former case we invert the inequality and add $\mathcal{D}(p^{n-1}) - \mathcal{D}(\hat{p})$ to arrive at

$$\mathcal{D}(p^n) - \mathcal{D}(\hat{p}) \leq (1 - \frac{\rho\sigma}{2\alpha})(\mathcal{D}(p^{n-1}) - \mathcal{D}(\hat{p})),$$

which recursively yields the required statement for all $n \leq n_0$. In the latter case we may assume without loss of generality that $n_0 = 0$ since we can shift the sequence if necessary. Thus for all $n \in \mathbb{N}_0$:

$$\mathcal{D}(p^n) - \mathcal{D}(p^{n+1}) \geq \frac{\rho\sigma}{2\Phi^2\alpha^2}(\mathcal{D}(p^n) - \mathcal{D}(\hat{p}))^2.$$

Invoking Lemma 4.6 with constant $c := \frac{\rho\sigma}{2\Phi^2\alpha^2}$ we obtain

$$\mathcal{D}(p^n) - \mathcal{D}(\hat{p}) \leq \frac{1}{cn + \frac{1}{\mathcal{D}(p^0) - \mathcal{D}(\hat{p})}} \leq \frac{1}{cn + \frac{1}{\Phi^2\alpha}} \leq \frac{1}{cn + \frac{\rho\sigma}{2\Phi^2\alpha^2}} = \frac{1}{c(n+1)}$$

since $0 \leq \sigma, \rho \leq 1$ and $\alpha \geq 1$, thereby showing the second inequality, which completes the proof.

5 Comparison

We conclude that in special cases the results obtained here are either in agreement with or may improve upon other known estimates. In particular, in the following we compare our findings with the ones in [30] and [7].

5.1 Gradient Method Framework [30]

In the special case of parallel decomposition, i.e. $\alpha = 1$, and exact local solutions, i.e. $\rho = 1$, the framework of [30] is applicable to our model and their estimate [30, Algorithm 4.1] reproduces ours. We show this by specializing and transforming their estimate.

Using notation from [30] we employ [30, Algorithm 4.1] by setting $E(u) = F(u) + G(u) := \mathcal{D}(u) + \chi_K(u)$, where $\chi_K(u) = 0$ if $u \in K$ and ∞ otherwise. The space decomposition is specified by the images of θ_k , $k = 1, \dots, M$, i.e. $V_k := \text{im } \theta_k \subset V$ with $R_k^* : V_k \rightarrow V$ then being the inclusion map. We chose to use exact local solvers, i.e. $\rho = 1$ in our notation, since it is not obvious to us how our notion of approximate minimization map to theirs. In particular, d_k and G_k are chosen as in [30, (4.3)] and $\omega := \omega_0 := 1$. We now verify [30, Assumptions 4.1 to 4.3] in order to apply [30, Theorem 4.7]. [30, Assumption 4.1] is fulfilled due to Lemmas 4.5 and 4.8 with $C_{0,K} := C_\theta \|\Lambda\| \sqrt{\|B^{-1}\|}$ and $q := 2$. We fulfill [30, Assumption 4.2] by choosing $\tau_0 := \frac{1}{N}$ (their τ corresponds to our σ). [30, Assumption 4.3] is trivialized in the case of exact local solvers. Applying [30, Theorem 4.7] with $C_{q,\tau} = 2$ and $\kappa = \frac{1}{\tau} C_\theta^2 \|\Lambda\|^2 \|B^{-1}\|$ yields

$$\mathcal{D}(p^1) - \mathcal{D}(\hat{p}) \leq (1 - \sigma(1 - \frac{1}{2}))(\mathcal{D}(p^0) - \mathcal{D}(\hat{p})) = (1 - \frac{\sigma}{2})(\mathcal{D}(p^0) - \mathcal{D}(\hat{p})) \quad (15)$$

if $\mathcal{D}(p^0) - \mathcal{D}(\hat{p}) \geq \tau R_{\hat{p}}^2 \kappa = \Phi^2$ and

$$\mathcal{D}(p^n) - \mathcal{D}(\hat{p}) \leq \frac{C_{q,r} R_{\hat{p}}^2 \kappa}{(n+1)^{q-1}} = \frac{2\Phi^2}{\sigma} (n+1)^{-1} \quad (16)$$

otherwise. Applying estimate (15) recursively and shifting the sequence by n_0 for the estimate (16) finally yields the formulation

$$\mathcal{D}(p^n) - \mathcal{D}(\hat{p}) \leq \begin{cases} (1 - \frac{\sigma}{2})^n (\mathcal{D}(p^0) - \mathcal{D}(\hat{p})) & \text{if } n \leq n_0 \\ \frac{2\Phi^2}{\sigma} (n - n_0 + 1)^{-1} & \text{if } n \geq n_0, \end{cases}$$

which is in agreement with Theorem 4.2.

5.2 Decomposition of the Rudin-Osher-Fatemi Model [7]

In order to compare with the convergence rate in [7], we specialize our model to their setting by choosing $V = H_0^{\text{div}}(\Omega)$, $\Lambda = \text{div} : V \rightarrow L^2(\Omega)$, $T = I : L^2(\Omega) \rightarrow L^2(\Omega)$, $\beta = 0$ (thus $B = I$) and $\rho = 1$. Next we introduce some notation from [7], namely $C_0, \delta > 0$ such that $\|\nabla \tilde{\theta}_i\|_{L^\infty} \leq \frac{C_0}{\delta}$ for $i = 1, \dots, M$, c.f. [7, (2.10)], $\zeta^0 := 2(\mathcal{D}(p^0) - \mathcal{D}(\hat{p}))$ (our \mathcal{D} has an additional factor of $\frac{1}{2}$) and $N_0 := \max_{x \in \Omega} |\{i \in \{1, \dots, M\} : x \in \Omega_i\}|$. Then [7, Theorem 3.1] and [7, Theorem 3.6] provide the following estimate:

$$\frac{1}{2} \|u^n - \hat{u}\|_{L^2}^2 \leq \mathcal{D}(p) - \mathcal{D}(\hat{p}) \leq Cn^{-1} \quad (17)$$

where $u^n := -\operatorname{div} p^n + g$, $\hat{u} := -\operatorname{div} \hat{p} + g$ and

$$C := \frac{1}{2} \zeta^0 \left(\frac{2}{\sigma} (2M + 1)^2 + 8\sqrt{2} C_0 \lambda |\Omega|^{\frac{1}{2}} (\zeta^0)^{-\frac{1}{2}} \frac{M\sqrt{N_0}}{\delta\sqrt{\sigma}} + \sqrt{2} - 1 \right)^2.$$

Note that we used our notation for M and σ .

In order to compare favorably in this setting, we slightly refine the estimate $\Phi_n \leq \Phi$ from the proof of Proposition 4.10. First, we quantify an estimate from the proof of Lemma 2.1. For all $p \in V$ we have

$$\begin{aligned} \sum_{i=1}^M \|\operatorname{div} \theta_i p\|_{L^2}^2 &\leq \sum_{i=1}^M \|\nabla \tilde{\theta}_i \cdot p + \tilde{\theta}_i \operatorname{div} p\|_{L^2}^2 \\ &\leq \sum_{i=1}^M \left((1 + \omega) \|\nabla \tilde{\theta}_i \cdot p\|_{L^2}^2 + (1 + \omega^{-1}) \|\tilde{\theta}_i \operatorname{div} p\|_{L^2}^2 \right) \\ &= (1 + \omega) \int_{\Omega} \sum_{i=1}^M |\nabla \tilde{\theta}_i \cdot p|^2 \, dx + (1 + \omega^{-1}) \int_{\Omega} \sum_{i=1}^M |\tilde{\theta}_i \operatorname{div} p|^2 \, dx \\ &\leq (1 + \omega) \int_{\Omega} \left(\sum_{i=1}^M |\nabla \tilde{\theta}_i|^2 \right) |p|^2 \, dx \\ &\quad + (1 + \omega^{-1}) \int_{\Omega} \left(\sum_{i=1}^M |\tilde{\theta}_i|^2 \right) |\operatorname{div} p|^2 \, dx \\ &\leq (1 + \omega) N_0 \|\nabla \tilde{\theta}_i\|_{L^\infty}^2 \|p\|_{L^2}^2 + (1 + \omega^{-1}) \|\operatorname{div} p\|_{L^2}^2 \\ &\leq (1 + \omega) N_0 \frac{C_0^2}{\delta^2} \|p\|_{L^2}^2 + (1 + \omega^{-1}) \|\operatorname{div} p\|_{L^2}^2, \end{aligned}$$

for any $\omega > 0$. The pointwise box-constraints $|p| \leq \lambda$ imply $\|p^n - \hat{p}\|_{L^2}^2 = \int_{\Omega} |p^n - \hat{p}|^2 \, dx \leq (2\lambda)^2 |\Omega|$. Combining this allows us to estimate

$$\begin{aligned} \Phi_n^2 &:= \sum_{i=1}^M \|\theta_i(p^n - \hat{p})\|_*^2 = \sum_{i=1}^M \|\operatorname{div} \theta_i(p^n - \hat{p})\|_{L^2}^2 \\ &\leq (1 + \omega) N_0 \frac{C_0^2}{\delta^2} \|p^n - \hat{p}\|_{L^2}^2 + (1 + \omega^{-1}) \|\operatorname{div}(p^n - \hat{p})\|_{L^2}^2 \\ &\leq (1 + \omega) \cdot 4\lambda^2 |\Omega| N_0 \frac{C_0^2}{\delta^2} + (1 + \omega^{-1}) \zeta^0 \\ &= \left(2\lambda |\Omega|^{\frac{1}{2}} N_0^{\frac{1}{2}} \frac{C_0}{\delta} + (\zeta^0)^{\frac{1}{2}} \right)^2 =: \tilde{\Phi}^2 \end{aligned}$$

by optimally choosing $\omega := (4\lambda^2 |\Omega| N_0 \frac{C_0^2}{\delta^2})^{-\frac{1}{2}} (\zeta^0)^{\frac{1}{2}}$. We therefore conclude that in this specific setting Theorem 4.2 holds true with Φ replaced by $\tilde{\Phi}$. Their and our estimate thus amount to

$$\frac{1}{2} \|u^n - \hat{u}\|^2 \leq C n^{-1},$$

$$\frac{1}{2}\|u^n - \hat{u}\|^2 \leq \frac{2\bar{\Phi}^2}{\sigma}\alpha^2(n - n_0 + 1)^{-1},$$

where for the lower estimate α and n_0 are defined as in Theorem 4.2 and $n \geq n_0$. Rewriting the involved constants,

$$\begin{aligned} C &= \left(\left(\frac{\sqrt{2}(2M+1)^2}{\sigma} + \sqrt{2} - 1 \right) \sqrt{\zeta^0} + 8 \frac{M}{\sqrt{\sigma}} \lambda |\Omega|^{\frac{1}{2}} \sqrt{N_0 \frac{C_0}{\delta}} \right)^2, \\ \frac{2\bar{\Phi}^2\alpha^2}{\sigma} &\leq \frac{2(1+\sigma M)^2}{\sigma} \left(2\lambda |\Omega|^{\frac{1}{2}} \sqrt{N_0 \frac{C_0}{\delta}} + \sqrt{\zeta^0} \right)^2 \\ &= \left(\sqrt{2} \frac{1+\sigma M}{\sqrt{\sigma}} \sqrt{\zeta^0} + 2\sqrt{2} \frac{1+\sigma M}{\sqrt{\sigma}} \lambda |\Omega|^{\frac{1}{2}} \sqrt{N_0 \frac{C_0}{\delta}} \right)^2, \end{aligned}$$

we see that $\frac{2\bar{\Phi}^2\alpha^2}{\sigma} \leq C$ by comparing the relevant terms before $\sqrt{\zeta^0}$ and $\lambda |\Omega|^{\frac{1}{2}} \sqrt{N_0 \frac{C_0}{\delta}}$ under the square separately using $0 < \sigma \leq 1$ and $M \geq 1$:

$$\begin{aligned} \sqrt{2} \frac{1+\sigma M}{\sqrt{\sigma}} &\leq \frac{\sqrt{2}}{\sqrt{\sigma}}(1+M) < \frac{\sqrt{2}(2M+1)^2}{\sigma} \leq \frac{\sqrt{2}(2M+1)^2}{\sigma} + \sqrt{2} - 1 \\ 2\sqrt{2} \frac{1+\sigma M}{\sqrt{\sigma}} &\leq 3 \frac{1+M}{\sqrt{\sigma}} < 4 \frac{2M}{\sqrt{\sigma}} = 8 \frac{M}{\sqrt{\sigma}}. \end{aligned}$$

Consequently, Theorem 4.2 provides a strictly better estimate than [7, Theorems 3.1, 3.6] both for sufficiently large $n \in \mathbb{N}$ and for all $n \in \mathbb{N}$ whenever $n_0 = 0$ (i.e. the initial guess is close enough). While we expect Theorem 4.2 to still be better than [7, Theorems 3.1, 3.6] for $n_0 > 0$, a complete comparison in that case seems to be more involved and remains to be done.

6 Surrogate Technique

A surrogate iteration substitutes minimization of one functional for minimization of different, simpler functionals at the cost of an additional iterative process. In particular one can substitute the minimization problem $\inf_{p \in K} \frac{1}{2} \|\Lambda p - T^*g\|_{B^{-1}}^2$ by the iteration

$$\inf_{p^{n+1} \in K} \frac{1}{2} \|\Lambda p^{n+1} - f^n\|_W^2, \quad f^n = \Lambda p^n - \frac{1}{\tau} B^{-1}(\Lambda p^n - T^*g),$$

producing iterates $(p^n)_{n \in \mathbb{N}}$ for some initialization $p^0 \in V$ that converge to the same minimizer, provided $\tau \in (\|B^{-1}\|, \infty)$. Though its properties have been studied extensively in e.g. [29], we will analyze it as a nested subalgorithm of our decomposition scheme for approximate minimization following the notion from Definition 3.1. The main motivation for the surrogate technique in our case is to rid the local problems from the dependence on the potentially costly operator B^{-1} .

To that end for $n \in \mathbb{N}_0$ we introduce an auxiliary functional $\mathcal{D}_i^{s,n}$ defined as

$$\mathcal{D}_i^{s,n}(v_i, w_i) := \mathcal{D}(p_{i-1}^n + (v_i - \theta_i p^n)) + \frac{1}{2} \|\Lambda(v_i - w_i)\|_{\tau I - B^{-1}}^2$$

with $\tau > \|B^{-1}\|$ for $v_i, w_i \in \theta_i K$ and $i = 1, \dots, M$, whereby $\|u\|_{\tau I - B^{-1}}^2 := \langle u, (\tau I - B^{-1})u \rangle_W$ for $u \in W$.

Algorithm 3 Surrogate approximation

Require: $N_{\text{sur}} \in \mathbb{N}$, $n \in \mathbb{N}_0$, $i \in \{1, \dots, M\}$, $p^n \in K$, $p_{i-1}^n \in K$

Ensure: $\tilde{v}_i^n \in \theta_i K$

- 1: $v_i^{n,0} = \theta_i p_{i-1}^n$
 - 2: **for** $\ell = 0, 1, \dots, N_{\text{sur}} - 1$ **do**
 - 3: $v_i^{n,\ell+1} \in \arg \min_{v_i \in \theta_i K} \mathcal{D}_i^{s,n}(v_i, v_i^{n,\ell})$
 - 4: **end for**
 - 5: $\tilde{v}_i^n = v_i^{n, N_{\text{sur}}}$
-

We note that the subproblems in Algorithm 3 can be written as

$$\begin{aligned} & \inf_{v_i \in \theta_i K} \mathcal{D}_i^{s,n}(v_i, v_i^{n,\ell}) \\ \iff & \inf_{v_i \in \theta_i K} \frac{1}{2} \|\Lambda(p_{i-1}^n + (v_i - \theta_i p^n)) - T^*g\|_{B^{-1}}^2 + \frac{1}{2} \|\Lambda(v_i - v_i^{n,\ell})\|_{\tau I - B^{-1}}^2 \\ \iff & \inf_{v_i \in \theta_i K} \frac{1}{2} \|\Lambda v_i - f_i^n\|_W^2, \end{aligned}$$

where $f_i^n = \Lambda v_i^{n,\ell} - \frac{1}{\tau} B^{-1}(\Lambda(p_{i-1}^n + (v_i^{n,\ell} - \theta_i p^n)) - T^*g)$. The dependence on the operator B^{-1} has thereby been moved into the preparation of fixed data f_i^n for every subproblem, while the subproblem itself for fixed f_i^n is independent of B^{-1} .

Algorithm 3 produces approximations \tilde{v}_i^n to be used in Algorithms 1 and 2. Following ideas from [29, Proposition 2.2] we show below, that the surrogate approximation converges linearly and any fixed number of surrogate iterations N_{sur} is enough to receive the convergence rate from Theorem 4.2 for the resulting combined algorithm.

Lemma 6.1. *Using notation and assumptions from Algorithm 3 the functional $\mathcal{D}_i^n : V_i \rightarrow \mathbb{R}$,*

$$\mathcal{D}_i^n(v) := \mathcal{D}(p_{i-1}^n - \theta_i p^n + v),$$

has quadratic growth in the sense that

$$\mathcal{D}_i^n(v) - \mathcal{D}_i^n(\hat{v}) \geq \frac{1}{2\|\tau I - B^{-1}\|\|B\|} \|\Lambda(v - \hat{v})\|_{\tau I - B^{-1}}^2$$

for any minimizer $\hat{v} \in \theta_i K$ of \mathcal{D}_i^n .

Proof Using Lemma 4.5 and optimality of $\hat{v} \in \theta_i K$ we see that

$$\mathcal{D}_i^n(v) - \mathcal{D}_i^n(\hat{v}) = \langle \mathcal{D}'(p_{i-1}^n + (\hat{v} - \theta_i p^n)), v - \hat{v}_i \rangle + \frac{1}{2} \|v - \hat{v}\|_*^2$$

$$\geq \frac{1}{2} \|\Lambda(v - \hat{v})\|_{B^{-1}}^2.$$

Further noting that $\tau I - B^{-1}$ is positive definite, since $\tau > \|B^{-1}\|$,

$$\|\Lambda(v - \hat{v})\|_{\tau I - B^{-1}}^2 \leq \|\tau I - B^{-1}\| \|\Lambda(v - \hat{v})\|_W^2 \leq \|\tau I - B^{-1}\| \|B\| \|\Lambda(v - \hat{v})\|_{B^{-1}}^2.$$

Combining both inequalities yields the statement. \square

Proposition 6.2. *Using notation and assumptions from Algorithm 3 and Lemma 6.1 the surrogate iterates $(v_i^{n,\ell})_\ell$ satisfy*

$$\mathcal{D}_i^n(v_i^{n,\ell}) - \mathcal{D}_i^n(v_i^{n,\ell+1}) \geq \eta (\mathcal{D}_i^n(v_i^{n,\ell}) - \mathcal{D}_i^n(\hat{v}_i^n))$$

for all $\ell \in \mathbb{N}$ and for any minimizer $\hat{v}_i^n \in \theta_i K$ of \mathcal{D}_i^n , $i \in \{1, \dots, n\}$, $n \in \mathbb{N}_0$, while $\eta \in (0, 1)$ is given by

$$\eta = \begin{cases} \frac{1}{4\|\tau I - B^{-1}\| \|B\|} & \text{if } \|\tau I - B^{-1}\| \|B\| \geq \frac{1}{2} \\ 1 - \|\tau I - B^{-1}\| \|B\| & \text{else.} \end{cases}$$

Proof Since $\mathcal{D}_i^{s,n}(v, w) = \mathcal{D}_i^n(v) + \frac{1}{2} \|\Lambda(w - v)\|_{\tau I - B^{-1}}^2$ we have

$$\begin{aligned} & \mathcal{D}_i^n(v_i^{n,\ell+1}) + \frac{1}{2} \|\Lambda(v_i^{n,\ell} - v_i^{n,\ell+1})\|_{\tau I - B^{-1}}^2 \\ &= \mathcal{D}_i^{s,n}(v_i^{n,\ell+1}, v_i^{n,\ell}) \\ &= \min_{v_i \in \theta_i K} \mathcal{D}_i^n(v_i) + \frac{1}{2} \|\Lambda(v_i^{n,\ell} - v_i)\|_{\tau I - B^{-1}}^2 \\ &\leq \min_{\mu \in [0,1]} \mathcal{D}_i^n((1 - \mu)v_i^{n,\ell} + \mu \hat{v}_i^n) + \frac{\mu^2}{2} \|\Lambda(v_i^{n,\ell} - \hat{v}_i^n)\|_{\tau I - B^{-1}}^2 \\ &\leq \min_{\mu \in [0,1]} (1 - \mu) \mathcal{D}_i^n(v_i^{n,\ell}) + \mu \mathcal{D}_i^n(\hat{v}_i^n) + \frac{\mu^2}{2} \|\Lambda(v_i^{n,\ell} - \hat{v}_i^n)\|_{\tau I - B^{-1}}^2, \end{aligned}$$

where we searched for the minimum along the line $v_i = (1 - \mu)v_i^{n,\ell} + \mu \hat{v}_i^n \in \theta_i K$, $\mu \in [0, 1]$, and used convexity afterwards. After reordering we use the quadratic growth property from Lemma 6.1 to see that

$$\begin{aligned} & \mathcal{D}_i^n(v_i^{n,\ell}) - \mathcal{D}_i^n(v_i^{n,\ell+1}) - \frac{1}{2} \|\Lambda(v_i^{n,\ell} - v_i^{n,\ell+1})\|_{\tau I - B^{-1}}^2 \\ &\geq \max_{\mu \in [0,1]} \mu (\mathcal{D}_i^n(v_i^{n,\ell}) - \mathcal{D}_i^n(\hat{v}_i^n)) - \frac{\mu^2}{2} \|\Lambda(v_i^{n,\ell} - \hat{v}_i^n)\|_{\tau I - B^{-1}}^2 \\ &\geq \max_{\mu \in [0,1]} (\mu - \mu^2 \|\tau I - B^{-1}\| \|B\|) (\mathcal{D}_i^n(v_i^{n,\ell}) - \mathcal{D}_i^n(\hat{v}_i^n)). \end{aligned}$$

Discarding the last term on the left-hand side and evaluating the maximum optimally at $\mu = \min\{1, \frac{1}{2\|\tau I - B^{-1}\| \|B\|}\} \in (0, 1]$ yields

$$\mathcal{D}_i^n(v_i^{n,\ell}) - \mathcal{D}_i^n(v_i^{n,\ell+1}) \geq \eta (\mathcal{D}_i^n(v_i^{n,\ell}) - \mathcal{D}_i^n(\hat{v}_i^n))$$

where $\eta \in (0, 1)$ is given by

$$\eta = \begin{cases} \frac{1}{4\|\tau I - B^{-1}\| \|B\|} & \text{if } \|\tau I - B^{-1}\| \|B\| \geq \frac{1}{2} \\ 1 - \|\tau I - B^{-1}\| \|B\| & \text{else.} \end{cases}$$

\square

Proposition 6.2 is sharp in the sense that for trivial $B^{-1} = I$ and minimizing $1 < \tau \rightarrow 1$, we recover the optimal factor $\eta \rightarrow 1$.

Lemma 6.3. *The surrogate iterates $(v_i^{n,\ell})_\ell$ from Algorithm 3 yield approximate solutions to the subproblems in the sense that*

$$\mathcal{D}_i^n(v_i^{n,0}) - \mathcal{D}_i^n(v_i^{n,\ell}) \geq (1 - (1 - \eta)^\ell)(\mathcal{D}_i^n(v_i^{n,0}) - \mathcal{D}_i^n(\hat{v}_i^n))$$

for any minimizer $\hat{v}_i^n \in \theta_i K$ of \mathcal{D}_i^n , $i \in \{1 \dots, M\}$, $n \in \mathbb{N}_0$ and $\eta \in (0, 1)$ defined as in Proposition 6.2.

Proof Elementary calculation using Proposition 6.2 yields a linear energy decrease

$$\begin{aligned} \mathcal{D}_i^n(v_i^{n,\ell+1}) - \mathcal{D}_i^n(\hat{v}_i^n) &= -(\mathcal{D}_i^n(v_i^{n,\ell}) - \mathcal{D}_i^n(v_i^{n,\ell+1})) + \mathcal{D}_i^n(v_i^{n,\ell}) - \mathcal{D}_i^n(\hat{v}_i^n) \\ &\leq -\eta(\mathcal{D}_i^n(v_i^{n,\ell}) - \mathcal{D}_i^n(\hat{v}_i^n)) + \mathcal{D}_i^n(v_i^{n,\ell}) - \mathcal{D}_i^n(\hat{v}_i^n) \\ &= (1 - \eta)(\mathcal{D}_i^n(v_i^{n,\ell}) - \mathcal{D}_i^n(\hat{v}_i^n)) \end{aligned}$$

which we use to find

$$\begin{aligned} \mathcal{D}_i^n(v_i^{n,0}) - \mathcal{D}_i^n(v_i^{n,\ell}) &= \mathcal{D}_i^n(v_i^{n,0}) - \mathcal{D}_i^n(\hat{v}_i^n) - (\mathcal{D}_i^n(v_i^{n,\ell}) - \mathcal{D}_i^n(\hat{v}_i^n)) \\ &\geq \mathcal{D}_i^n(v_i^{n,0}) - \mathcal{D}_i^n(\hat{v}_i^n) - (1 - \eta)^\ell(\mathcal{D}_i^n(v_i^{n,0}) - \mathcal{D}_i^n(\hat{v}_i^n)) \\ &\geq (1 - (1 - \eta)^\ell)(\mathcal{D}_i^n(v_i^{n,0}) - \mathcal{D}_i^n(\hat{v}_i^n)). \end{aligned}$$

□

Finally, combining Theorem 4.2 with Lemma 6.3 then immediately yields the following corollary.

Corollary 6.4. *Algorithms 1 and 2 with subproblems solved using Algorithm 3 converge in the sense that $\mathcal{D}(p^n) \rightarrow \mathcal{D}(\hat{p})$. Furthermore*

$$\mathcal{D}(p^n) - \mathcal{D}(\hat{p}) \leq \begin{cases} (1 - \frac{\rho\sigma}{2\alpha})^n (\mathcal{D}(p^0) - \mathcal{D}(\hat{p})) & \text{if } n \leq n_0 \\ \frac{2\Phi^2}{\rho\sigma} \alpha^2 (n - n_0 + 1)^{-1} & \text{if } n \geq n_0, \end{cases}$$

where $\alpha := 1 + M\sigma\sqrt{2 - \rho + 2\sqrt{1 - \rho}}$ for Algorithm 2 and $\alpha := 1$ for Algorithm 1, $\Phi := \sqrt{\|B^{-1}\| \|\Lambda\| C_\theta R_{\hat{p}}}$, $n_0 := \min\{n \in \mathbb{N}_0 : \mathcal{D}(p^n) - \mathcal{D}(\hat{p}) < \Phi^2 \alpha\}$ and

$$\rho = (1 - (1 - \eta)^{N_{sur}}), \quad \eta = \begin{cases} \frac{1}{4\|\tau I - B^{-1}\| \|B\|} & \text{if } \|\tau I - B^{-1}\| \|B\| \geq \frac{1}{2} \\ 1 - \|\tau I - B^{-1}\| \|B\| & \text{else.} \end{cases}$$

for any fixed number of inner surrogate iterations $N_{sur} \in \mathbb{N}$.

Remark 6.5. *In Algorithm 3 we specify a fixed number of surrogate iterations over all subdomain problems, i.e. N_{sur} is the same in each subdomain. However, one may indeed make N_{sur} dependent on Ω_i leading to $N_{sur,i}$ for*

$i = 1, \dots, M$. Note that this does not change the statements in Proposition 6.2 and Lemma 6.3 as these estimates only concern the subproblems separately. Moreover, the estimate in Lemma 6.3 is the weaker the smaller $\ell \in \mathbb{N}$ is, since $1 - (1 - \eta)^a > 1 - (1 - \eta)^b$ for $a > b$ as $1 - \eta \in (0, 1)$. Together with this observation we obtain that in the case of subdomain dependent inner surrogate iterations Corollary 6.4 then holds with replacing N_{sur} by $\min_{i \in \{1, \dots, M\}} N_{sur, i}$, i.e. by the minimal number of inner surrogate iterations over all subdomains.

Remark 6.6. The above presented algorithms and its analysis is not restricted to problem (4) and also holds for more general problems of the following type

$$\inf_{p \in K} \left\{ \tilde{\mathcal{D}}(p) := \frac{1}{2} \|\Lambda p - f\|_{B^{-1}}^2 \right\}, \quad (18)$$

where $\Lambda : V \rightarrow W$ is a bounded linear operator, V, W are real Hilbert spaces, $B^{-1} : W \rightarrow W$ a positive definite self-adjoint bounded linear operator, $K \subset V$ a closed convex set, $f \in W$, and $\|q\|_{B^{-1}}^2 := \langle B^{-1}q, q \rangle_W$ for $q \in W$. Assuming coercivity of $\tilde{\mathcal{D}}$ ensures the existence of a solution of (18).

In particular we obtain the same convergence order results for (18) as for (4), i.e. Theorem 4.2 and Corollary 6.4 also hold in case of (18).

7 Semi-Implicit Dual Algorithm

Solution strategies for solving (4) are especially relevant in our decomposition setting of Algorithms 1 and 2, since we have to solve subproblems (10) of the same general form. One specific such algorithm is the semi-implicit Lagrange multiplier method due to Chambolle [6] which solves (4) for the special case $B = I$. While [6] uses finite differences, we present the algorithm in a Hilbert space setting and for more general B .

As in (4) let $K := \{p \in V : |p|_F \leq \lambda\}$ denote the set of feasible dual variables. Similar to [6] there exists a Lagrange multiplier $\mu \in L^\infty(\Omega)$ corresponding to the constraint in K , c.f. [18, Theorem 1.6], such that $p \in V$ is a solution of (4) if and only if

$$0 = \Lambda^* B^{-1}(\Lambda p - T^*g) + \mu p \quad (19)$$

with $\mu \geq 0$, $|p|_F \leq \lambda$ and $\frac{\mu}{2}(|p|_F^2 - \lambda^2) = 0$ holds. Here μp is to be understood as pointwise multiplication.

Recall that $\lambda > 0$. Observing that in a pointwise sense $\mu = 0$ implies $\xi := \Lambda^* B^{-1}(\Lambda p - T^*g) = 0$ and $\mu > 0$ implies $|p|_F = \lambda$ almost everywhere, we deduce from condition (19), that in either case $\mu = \frac{|\xi|_F}{\lambda}$. Thus (19) becomes

$$0 = \xi + \frac{|\xi|_F}{\lambda} p.$$

The semi-implicit iterative method then uses for some starting value $p^0 \in K$ and stepsize $\tau > 0$ iterates $(p^n)_{n \in \mathbb{N}_0} \subset V$ satisfying

$$p^{n+1} = p^n - \tau(\xi^n + \frac{|\xi^n|_F}{\lambda} p^{n+1}), \quad (20)$$

where $\xi^n := \Lambda^* B^{-1}(\Lambda p^n - T^* g)$, $n \in \mathbb{N}_0$. Solving (20) for p^{n+1} then yields Algorithm 4.

Algorithm 4 Semi-implicit dual multiplier method [6]

Require: $p^0 \in K$ and $\tau \in (0, \frac{1}{\|\Lambda^* B^{-1} \Lambda\|})$

- 1: **for** $n = 0, 1, 2, \dots$ **do**
 - 2: $\xi^n = \Lambda^* B^{-1}(\Lambda p^n - T^* g)$
 - 3: $p^{n+1} = \lambda \frac{p^n - \tau \xi^n}{\lambda + \tau |\xi^n|_F}$
 - 4: **end for**
-

Before we prove convergence of Algorithm 4 in the upcoming Theorem 7.2, let us first make some comments on Algorithm 4.

Remark 7.1. *Regarding Algorithm 4, take note of the following:*

- *In the trivial case $\lambda = 0$ one sets $p^{n+1} = 0$.*
- *If B^{-1} is a local operator, the computation of ξ^n and p^{n+1} are both local. They can therefore be merged together and carried out in parallel over the whole domain.*
- *One may solve the decomposition subproblems (10) by replacing K with $\theta_i K$ and λ with the pointwise function $\theta_i \lambda$.*
- *A more explicit bound for the maximum stepsize τ to still analytically ensure convergence is given by*

$$\|\Lambda^* B^{-1} \Lambda\| \leq \|\nabla\|^2 \|B^{-1}\|.$$

For finite differences as used in this paper (see Definition 8.1 below) we have [6]

$$\|\nabla_h\|^2 \leq 8.$$

Theorem 7.2 (c.f. [6, Theorem 3.1]). *Let $p^0 \in K$. Then Algorithm 4 generates a sequence $(p^n)_{n \in \mathbb{N}_0} \subset K$ such that $\mathcal{D}(p^n) \rightarrow \mathcal{D}(\hat{p})$ for $n \rightarrow \infty$ if V is finite dimensional, where $\hat{p} \in K$ is a minimizer of (4).*

Proof We follow along the lines of [6, Theorem 3.1]. Notice that $|p^0|_F \leq \lambda$ and thus inductively

$$|p^{n+1}|_F \leq \lambda \frac{|p^n|_F + \tau |\xi^n|_F}{\lambda + \tau |\xi^n|_F} \leq \lambda,$$

i.e. $p^n \in K$ for all $n \in \mathbb{N}$. Let $F : V \rightarrow V$ denote the iteration function of Algorithm 4, such that $p^{n+1} = F(p^n)$, $n \in \mathbb{N}_0$. Any fixed point of F or equivalently of (20) satisfies

the stationary point condition (19) per construction and, since \mathcal{D} is convex, will be a minimizer of (4).

Denote $\eta^n := \frac{1}{\tau}(p^n - p^{n+1})$ and bound the energy difference

$$\begin{aligned}
 \mathcal{D}(p^n) - \mathcal{D}(p^{n+1}) &= -\frac{1}{2}\|p^n - p^{n+1}\|_*^2 + \langle \mathcal{D}'(p^n), p^n - p^{n+1} \rangle \quad (\text{Lemma 4.5 (i)}) \\
 &= -\frac{\tau^2}{2}\|\eta^n\|_*^2 + \tau\langle \xi^n, \eta^n \rangle \\
 &= \frac{\tau}{2}(\|\eta^n\|^2 - \tau\|\eta^n\|_*^2) + \tau\langle \xi^n - \frac{1}{2}\eta^n, \eta^n \rangle \\
 &= \frac{\tau}{2}(\|\eta^n\|^2 - \tau\|\eta^n\|_*^2) + \frac{\tau}{2}\langle \xi^n - \frac{|\xi^n|_F}{\lambda}p^{n+1}, \xi^n + \frac{|\xi^n|_F}{\lambda}p^{n+1} \rangle \\
 &\quad (\text{applying (20)}) \\
 &= \frac{\tau}{2}(\|\eta^n\|^2 - \tau\langle \Lambda^* B \Lambda \eta^n, \eta^n \rangle) + \frac{\tau}{2}(\|\xi^n\|^2 - \|\frac{|\xi^n|_F}{\lambda}p^{n+1}\|^2) \\
 &\geq \frac{\tau}{2}(1 - \tau\|\Lambda^* B^{-1} \Lambda\|)\|\eta^n\|^2 + \frac{\tau}{2}\|\xi^n\|^2(1 - \|\frac{|p^{n+1}|_F}{\lambda^2}\|_{L^\infty}) \\
 &\geq \frac{1}{2\tau}(1 - \tau\|\Lambda^* B^{-1} \Lambda\|)\|p^n - p^{n+1}\|^2.
 \end{aligned}$$

We see that as long as $\tau < \|\Lambda^* B^{-1} \Lambda\|^{-1}$, the sequence $(\mathcal{D}(p^n))_{n \in \mathbb{N}_0}$ is non-increasing and thus, since it is non-negative, also convergent. The feasible set $K \subset V$ is closed and bounded, see [13, Lemma 3.4], and compact since V is finite dimensional. Consequently there exists a convergent subsequence $(q^n)_{n \in \mathbb{N}} \subset (p^n)_{n \in \mathbb{N}} \subset K$, $q^n \rightarrow q \in K$ and with continuity of F we get $F(q^n) \rightarrow F(q)$. Using the estimate above and the convergence of energies we see that for some $c > 0$ we have $c\|q^n - F(q^n)\|^2 \leq \mathcal{D}(q^n) - \mathcal{D}(F(q^n)) \rightarrow 0$ and therefore the limit needs to be a fixed point, $q = F(q)$, and thus a minimizer of (4). \square

We note that Theorem 7.2 guarantees the convergence to a minimal dual energy, which allows us to reconstruct the optimal primal solution due to Proposition 4.3. It does, however, not guarantee convergence of the dual iterates $(p^n)_{n \in \mathbb{N}}$ themselves.

8 Numerical Experiments

Let for $a, b \in \mathbb{Z}^d$ the discrete domain be given by

$$\Omega_h := \Omega_{h,[a,b]} := \{x = (x_1, \dots, x_d) \in \mathbb{Z}^d : a \leq x \leq b\} \subset \mathbb{Z}^d.$$

Computer images given by an array $A \in [0, 1]^{n_1 \times \dots \times n_d}$, $n = (n_1, \dots, n_d) \in \mathbb{N}^d$ of intensity values between 0 (black) and 1 (white) are then mapped to a discrete function $u_h : \Omega_{h,[1,n]} \rightarrow \mathbb{R}$ by defining $u_h(x) := A_x$.

Definition 8.1 (Finite Difference Operators). *For $u_h : \Omega_h \rightarrow \mathbb{R}^m$ and $p_h = (p_{h,1}, \dots, p_{h,d}) : \Omega_h \rightarrow \mathbb{R}^{d \times m}$ let forward differences $\partial_{h,k}^+ : \Omega_h \rightarrow \mathbb{R}^m$ and backward differences $\partial_{h,k}^- : \Omega_h \rightarrow \mathbb{R}^m$ be given by*

$$\partial_{h,k}^+ u_h(x) := \begin{cases} 0 & \text{if } x_k = b_k, \\ u_h(x + he^k) - u_h(x) & \text{else,} \end{cases},$$

$$\partial_{h,k}^- u_h(x) := \begin{cases} u_h(x) & \text{if } x_k = a_k, \\ -u_h(x - he^k) & \text{if } x_k = b_k, \\ u_h(x) - u_h(x - he^k) & \text{else,} \end{cases}$$

where $e^k \in \mathbb{N}^d$ denotes the k -th unit vector, $k = 1, \dots, d$. The discrete gradient $\nabla_h u_h : \Omega_h \rightarrow \mathbb{R}^{d \times m}$ and discrete divergence $\operatorname{div}_h p_h : \Omega_h \rightarrow \mathbb{R}^m$ are then defined as

$$\nabla_h u_h := (\partial_{h,k}^+ u_h)_{k=1}^d, \quad \operatorname{div}_h p_h := \sum_{k=1}^d \partial_{h,k}^- p_{h,k}.$$

For a given discrete overlap $r \in \mathbb{N}$ and a desired number of domains $M \in \mathbb{N}$ we first define a discrete covering of Ω_h in dimension $d = 1$. Let $s := |b - a|$ be the diameter of Ω_h , i.e. its length. Define M approximately equal integer sublengths given recursively by

$$a_i := \left\lfloor \frac{s + (M-1)r - \sum_{j=1}^{i-1} (a_j - r)}{M - (i-1)} \right\rfloor, \quad i = 1, \dots, M.$$

These give rise to the subdomains

$$\Omega_{h,i} := \{b_i, b_i + 1, \dots, b_i + a_i\}, \quad b_i := \sum_{j=1}^{i-1} (a_j - r), \quad i = 1, \dots, M$$

of diameter a_i and the partition functions $\theta_{h,i} : \Omega_h \rightarrow [0, 1]$ by

$$\theta_{h,i}(x) := \min \left\{ 1, \frac{1}{r} \operatorname{dist}(x, [0, s] \setminus [b_i, b_i + a_i]) \right\},$$

where dist is the (Euclidean) distance function. The above construction in one dimension yields M discrete subdomains $\Omega_{h,i}$ and a corresponding partition of unity $\theta_{h,i}$ for a discrete domain Ω_h of any size provided M and r are chosen such that $a_i \geq 2r$.

Higher dimensions $d > 1$ are realized through a standard tensor-product formulation based on the above construction, yielding $M = \prod_{k=1}^d M_k$ subdomains with overlaps $r = (r_1, \dots, r_d)$.

In all our decomposition examples we use Algorithm 4 as a subproblem solver if not specified otherwise and choose its stepsize $\tau = \frac{1}{8\|B^{-1}\|}$ in accordance with Remark 7.1.

The source code for all following numerical examples has been made available under a permissive license [12].

8.1 Convergence

We numerically verify the theoretical sublinear convergence properties of Algorithm 1 and Algorithm 2 due to Theorem 4.2 for three different applications, i.e. image denoising, image inpainting and estimating the optical flow.

For each application described below we compare Algorithm 4 on the global, non-decomposed problem and the decomposition Algorithms 1 and 2. For the global algorithm we abort after 10^6 iterations, while for the decomposition algorithms with Algorithm 4 as a subalgorithm solver, we abort after 10,000 outer iterations and each subalgorithm after 100 inner iterations. For a fair comparison we denote with $k \in \mathbb{N}$ the outer iterations of Algorithms 1 and 2 and the iterations of the global algorithm inversely scaled by the number of inner iterations of the decomposition algorithms, that is

$$k = \begin{cases} n & \text{if Algorithm 1 or Algorithm 2 is used;} \\ \frac{n}{100} & \text{if Algorithm 4 is used as global algorithm.} \end{cases}$$

All three algorithms are initialized using $p^0 = 0$. For both Algorithms 1 and 2 in each outer iteration n the subalgorithm on the i -th subdomain is initialized with the current subdomain view $\theta_i p_{i-1}^n \in \theta_i K$.

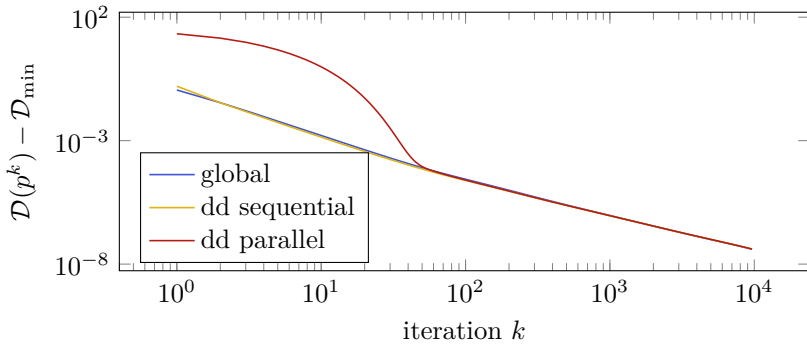
In each case we downsample input images to a small size of 48×32 pixels and decompose the domain into $M = 2 \cdot 2$ subdomains with an overlap of $r_1 = r_2 = 5$ pixels in order to make a very high number of iterations timely feasible. For Algorithm 2 and Algorithm 1 we use the largest allowable value of σ , i.e. $\sigma = 1$ and $\sigma = \frac{1}{4}$ respectively.

The three applications are realized by making use of Proposition 1.1 and setting data g , operator T and model parameters λ, β therein as follows.

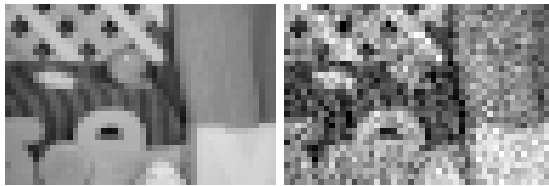
Denoising We start with a ground truth image \tilde{g} and generate an artificially noisy input $g = \tilde{g} + \eta$, where η denotes zero-mean additive Gaussian noise with variance 0.1. Setting $T = I$, and choosing model parameters $\lambda = 0.1$, $\beta = 0$ we apply the respective algorithm to obtain the denoised output u .

Inpainting Starting with a ground truth image \tilde{g} we artificially mask each pixel with probability $\frac{1}{2}$ by setting its value to 0 (black) to receive a corrupted input image g . Denoting by $A \subseteq \Omega$ the masked area we set $T = \mathbf{1}_{\Omega \setminus A}$ where $\mathbf{1}_{\Omega \setminus A}$ is the indicator function on $\Omega \setminus A$ while the model parameters are chosen to be $\lambda = 5 \cdot 10^{-2}$, $\beta = 1 \cdot 10^{-3}$.

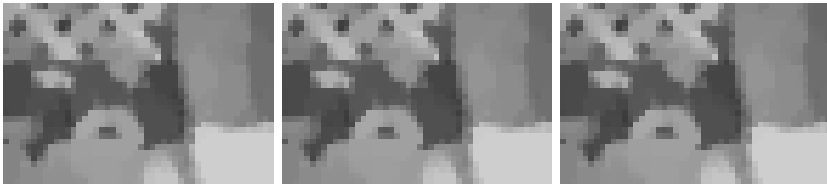
Optical flow estimation Given two grayscale images $g_0, g_1 : \Omega \rightarrow [0, 1]$ we estimate their vector-valued optical flow displacement field u by setting the difference $g = g_0 - g_1$ as input data and T using $Tu = \nabla g_1 \cdot u$. This formulation is the linear approximation of the brightness constancy constraint suitable for small displacements and may be found in [3, (5.81)]. Model parameters are set to $\lambda = 2 \cdot 10^{-3}$, $\beta = 1 \cdot 10^{-3}$. We visualize the optical flow field u and the benchmark-provided ground truth as a color-coded image following [4].



(a) energy



(b) ground truth image (c) noisy input image

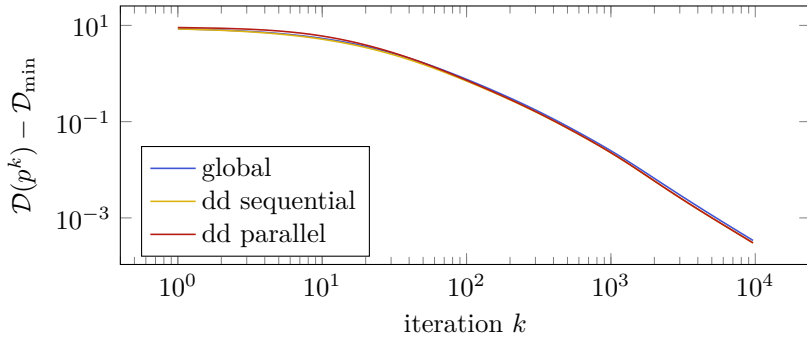


(d) denoised output image, global (e) denoised output image, dd sequential (f) denoised output image, dd parallel

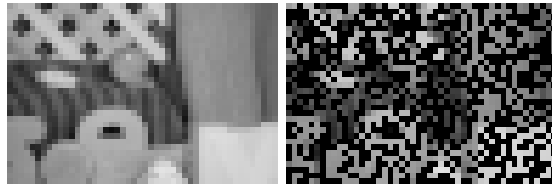
Fig. 1: denoising: convergence of energy and results

For each of the applications we denote by \mathcal{D}_{\min} the minimum energy obtained by running the global Algorithm 4 for a maximum of 10^7 iterations. For denoising, inpainting and optical flow estimation we determined $\mathcal{D}_{\min} \approx 456.61$, $\mathcal{D}_{\min} \approx 226.37$ and $\mathcal{D}_{\min} \approx 6.74 \cdot 10^{-2}$ respectively. The energy values over all iteration for the three algorithms and each application are plotted in Figures 1 to 3 together with respective input and output images.

We observe in Figure 1 similar behaviour as in [7], i.e. the sequential decomposition has a slight edge on the global algorithm due to domain-overlap, while the energy curve of the parallel averaging algorithm displays a characteristic bulge in the beginning. In Figures 2 and 3 the performance difference during the iterations between the sequential and parallel algorithm is less visible for



(a) energy



(b) ground truth image (c) corrupted input image



(d) inpainted output image, global (e) inpainted output image, dd sequential (f) inpainted output image, dd parallel

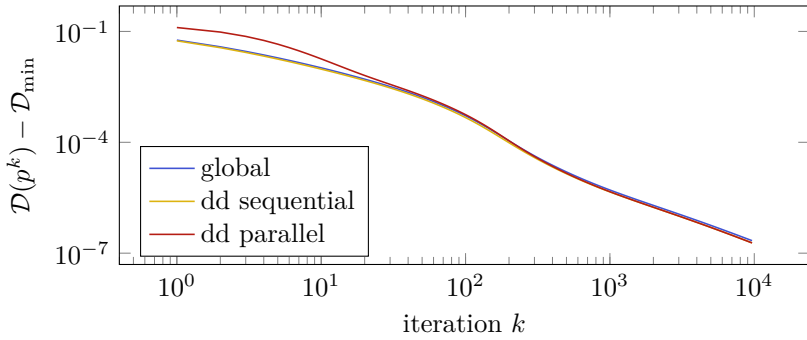
Fig. 2: inpainting: convergence of energy and results

both inpainting and optical flow estimation. In all cases the domain decomposition algorithms converge at a sublinear rate comparable to the respective global algorithm.

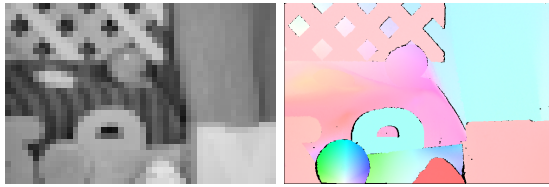
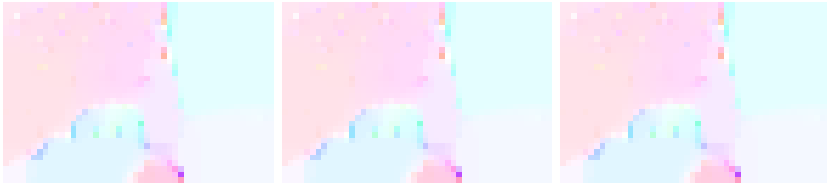
8.2 Surrogate

For local operators B we compare (i) nesting the surrogate iteration (Algorithm 3) within domain decomposition and (ii) nesting domain decomposition within a global surrogate iteration. Note that for $B = I$, $\tau \rightarrow 1$ and a single surrogate iteration both of these are identical.

We use the optical flow problem with frames of original size 584×388 pixels and model parameters $\beta = 1 \cdot 10^{-3}$, $\lambda = 1 \cdot 10^{-2}$. The number of subdomains is $M = 4 \cdot 4$ with larger overlap $r_1 = r_2 = 50$ pixels corresponding to the larger image size. We perform for both ways of nesting 50 iterations of the



(a) energy

(b) first image f_0 of image sequence (c) optical flow ground truth from [4] (original resolution)

(d) computed optical flow, global (e) computed optical flow, dd sequential (f) computed optical flow, dd parallel

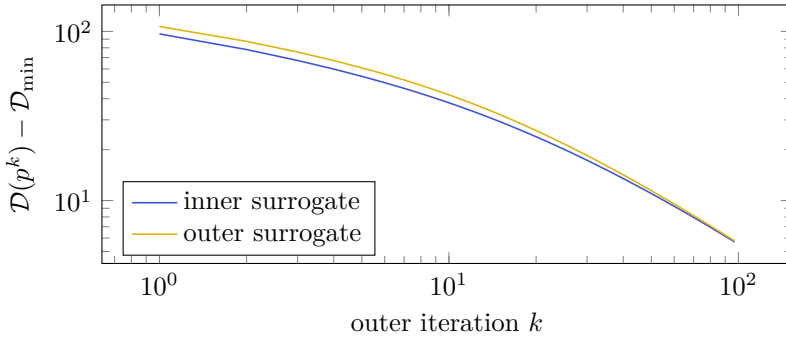
Fig. 3: optical flow: convergence of energy and results

inner algorithm and stop the whole algorithm after 100 outer iterations. We estimate the minimal energy $\mathcal{D}_{\min} \approx 107.57$ by running Algorithm 4 for 50,000 iterations.

Both nestings perform similarly as can be seen in Figure 4, while nesting the surrogate iteration within the domain decomposition has a slight edge. This can be attributed to additional evaluations of B in regions of overlap.

8.3 Wavelet Transformation

To demonstrate feasibility of our method even for global operators, we aim to apply it to the reconstruction of corrupted wavelet coefficients. To that end we first define the Wavelet transform T^∞ in a way convenient to us for working with arbitrarily sized images.



(a) energy

Fig. 4: Comparison of outer and inner surrogate, 50 inner iterations per domain decomposition iteration, one single inner iteration per surrogate iteration

Denote $\Omega_s := \Omega_{h,[1,s]}$ for $s \in \mathbb{N}_0^d$ and let $k = k(s) \in \mathbb{N}_0^d$ be such that $2k \leq s \leq 2k + 1$. We define the d -dimensional n -th level discrete Haar wavelet transform $T^n : \mathbb{R}^{\Omega_s} \rightarrow \mathbb{R}^{\Omega_s}$ recursively by $T^0 := I$ and for $n \geq 1$ by

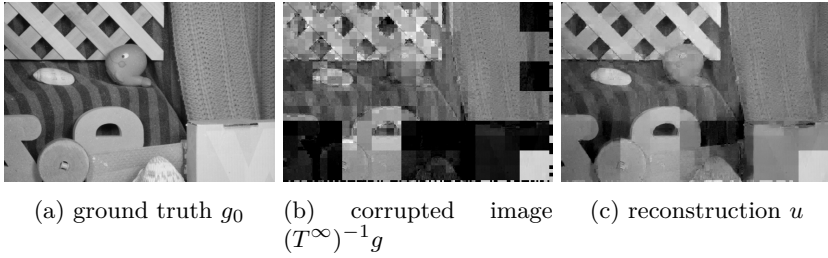
$$(T^n u)(\alpha \cdot k + x) := \begin{cases} (T^{n-1} T_0 u|_{\Omega_{2k}})(x) & \text{if } \alpha = 0, k \geq 1, \\ (T_\alpha u|_{\Omega_{2k}})(x) & \text{if } 0 \neq \alpha \leq 1, k \geq 1, \\ u(\alpha \cdot k + x) & \text{else,} \end{cases}$$

for all $\alpha \cdot k + x \in \Omega_s$, where $u : \Omega_s \rightarrow \mathbb{R}$, $\alpha, x \in \mathbb{N}^d$, $x \leq k$ and the transformation $T_\alpha : \mathbb{R}^{\Omega_{2k}} \rightarrow \mathbb{R}^{\Omega_k}$ on the orthant indicated by $\alpha \in \{0, 1\}^d$ is given by

$$(T_\alpha u)(x) := 2^{-\frac{d}{2}} \sum_{\substack{\beta \in \mathbb{N}_0^d \\ \beta \leq 1}} (-1)^{|\alpha \cdot \beta|} u(2(x-1) + 1 + \beta)$$

for all $x \in \mathbb{N}^d$, $x \leq k$. Since $T_\alpha : \mathbb{R}^{\Omega_{2k}} \rightarrow \mathbb{R}^{\Omega_k}$ halves the size and for $s \leq 1$ we have $T^n = I$ for any $n \in \mathbb{N}$, the operator T^n becomes idempotent for large enough n and we thus conveniently denote by $T^\infty := \lim_{n \rightarrow \infty} T^n$ the full wavelet transform.

We realize the application for wavelet inpainting by again making use of Proposition 1.1 and define data g , operator T and model parameters λ, β therein as follows. We start out with a ground truth image $g_0 \in \mathbb{R}^{\Omega_s}$ and compute artificially corrupted wavelet data $g = Tg_0 := RT^\infty g_0 \in \mathbb{R}^{\Omega_s}$ using an operator R as follows. We select a random subset $J \subset \Omega_s$ by choosing every element of Ω_s with probability $\frac{1}{2}$ and define for such fixed J the operator

**Fig. 5:** wavelet inpainting

$R = R_J : \mathbb{R}^{\Omega_s} \rightarrow \mathbb{R}^{\Omega_s}$ by

$$(Ru)(x) = \begin{cases} u(x) & \text{if } x \notin J, \\ 0 & \text{if } x \in J. \end{cases}$$

For model parameters we use $\lambda = 2 \cdot 10^{-2}$ and $\beta = 1 \cdot 10^{-3}$.

We decompose the domain into $M = 4 \cdot 4$ domains with an overlap of $r_1 = r_2 = 5$ pixels and apply Algorithm 2 with Algorithm 3 as a nested subalgorithm. We use $N_{\text{sur}} = 1$ surrogate iterations, 1,000 iterations for the innermost solver and stop the outer decomposition algorithm after just 100 iterations. In Figure 5 we can see the used ground truth g_0 , the corrupted image visualized as a naive reconstruction $(T^\infty)^{-1}g$ of the corrupted wavelet data g and the result of our wavelet inpainting u . Even in regions where bigger chunks of the corrupted image are lost, wavelet inpainting manages to reconstruct those structures which were preserved by other wavelet coefficients.

8.4 Parallel scaling

Algorithms 1 and 2 allow for a parallel implementation in a domain decomposition setting. Indeed, while the subproblems of Algorithm 1 are independent and may be executed in parallel without additional consideration, Algorithm 2 can be parallelized by applying the algorithm on colored classes of subdomains as in [7] and calculating the solution on a single colored class of disjoint subdomains in parallel.

We test a parallel implementation of Algorithm 2 using the same coloring technique from [7]. We use $M = 6 \cdot 6$ colored subdomains and otherwise the same parameters and image data as in the surrogate comparison above. This means that we have a maximum limit of 9 disjoint subproblems which can be scheduled in parallel. We execute the parallel algorithm with 1, 2, 4 and 8 workers respectively on a Intel(R) Core(TM) i7-5820K CPU @ 3.30GHz (6 cores, 12 processing units) and terminate after reaching an energy of 130.0.

In Figure 6 we can see that a parallel implementation can bring about runtime savings when increasing the number of parallel workers. The runtime

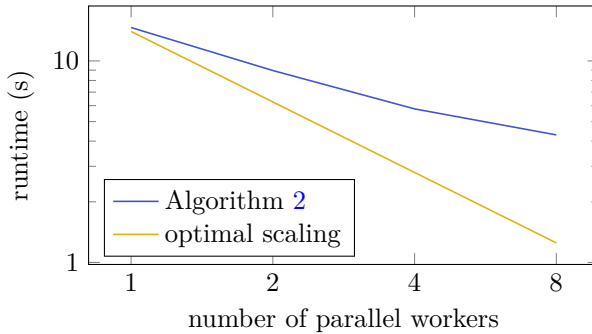


Fig. 6: time scaling behaviour for the parallel implementation of Algorithm 2 with regard to the number of parallel workers

behaves almost inversely linear to the number of workers up to number of available processor cores, though the constant factor is not optimal. We attribute this to the data preparation and communication steps that are carried out on a single worker and apparently do not scale well in this implementation.

9 Conclusion

We have seen that it is possible to improve the domain decomposition convergence rate results from [7] by making use of different proof techniques from alternating minimization. Since as in [7] Algorithm 2 has a slight advantage over Algorithm 1 in terms of iteration count, it suggests that there is still room for improvement of α in Theorem 4.2 in the sequential case.

We could easily apply Algorithms 1 and 2 to a wider range of local image processing tasks, namely inpainting and optical flow estimation, while global operators could only be decomposed by means of the surrogate technique, which incurred an additional cost. When considering the total number of iterations of the inner subalgorithm, Algorithms 1 and 2 did not differ substantially in terms of convergence speed from the global one, i.e. not decomposing the problem, which suggests a minor overhead of the decomposition method. A runtime improvement is only to be expected by parallel execution of the sub-problems which we managed to verify in a parallel implementation. Using the decomposition methods in a memory-constrained computing environment is expected to be possible.

Acknowledgement

This work was partly funded by the Ministerium für Wissenschaft, Forschung und Kunst of Baden-Württemberg (Az: 7533.-30-10/56/1) through the RISC-project “Automatische Erkennung von bewegten Objekten in hochauflösenden Bildsequenzen mittels neuer Gebietszerlegungsverfahren” and by Deutsche

Forschungsgemeinschaft (DFG, German Research Foundation) under Germany's Excellence Strategy – EXC 2075 – 390740016.

References

- [1] L. Ambrosio, N. Fusco, and D. Pallara. *Functions of Bounded Variation and Free Discontinuity Problems*. Oxford Mathematical Monographs. The Clarendon Press, Oxford University Press, New York, 2000.
- [2] H. Attouch, G. Buttazzo, and G. Michaille. *Variational Analysis in Sobolev and BV Spaces*. MOS-SIAM Series on Optimization. Mathematical Optimization Society and Society for Industrial and Applied Mathematics, Philadelphia, PA, second edition, 2014.
- [3] G. Aubert and P. Kornprobst. *Mathematical Problems in Image Processing*, volume 147 of *Applied Mathematical Sciences*. Springer, New York, second edition, 2006. Partial differential equations and the calculus of variations, With a foreword by Olivier Faugeras.
- [4] S. Baker, D. Scharstein, J. P. Lewis, S. Roth, M. J. Black, and R. Szeliski. A database and evaluation methodology for optical flow. *International Journal of Computer Vision*, 92(1):1–31, 2011.
- [5] J. W. Both. On the rate of convergence of alternating minimization for non-smooth non-strongly convex optimization in Banach spaces. *Optimization Letters*, 16(2):729–743, 2022.
- [6] A. Chambolle. An algorithm for total variation minimization and applications. *Journal of Mathematical Imaging and Vision*, 20(1-2):89–97, 2004.
- [7] H. Chang, X.-C. Tai, L.-L. Wang, and D. Yang. Convergence rate of overlapping domain decomposition methods for the Rudin–Osher–Fatemi model based on a dual formulation. *SIAM Journal on Imaging Sciences*, 8(1):564–591, 2015.
- [8] V. Dolean, P. Jolivet, and F. Nataf. *An Introduction to Domain Decomposition Methods: Algorithms, Theory, and Parallel Implementation*. SIAM, Philadelphia, PA, 2015.
- [9] M. Fornasier, Y. Kim, A. Langer, and C.-B. Schönlieb. Wavelet decomposition method for L_2 /TV-image deblurring. *SIAM Journal on Imaging Sciences*, 5(3):857–885, 2012.
- [10] M. Fornasier, A. Langer, and C.-B. Schönlieb. A convergent overlapping domain decomposition method for total variation minimization. *Numerische Mathematik*, 116(4):645–685, 2010.
- [11] M. Fornasier and C.-B. Schönlieb. Subspace correction methods for total variation and l_1 -minimization. *SIAM J. Numer. Anal.*, 47(5):3397–3428, 2009.
- [12] S. Hilb. DualTVDD: Dual total variation decomposition algorithm and related tools, 2021. <https://gitlab.mathematik.uni-stuttgart.de/stephan.hilb/DualTVDD.jl>.
- [13] S. Hilb, A. Langer, and M. Alkämper. A primal-dual finite element

- method for scalar and vectorial total variation minimization. Submitted, 2022.
- [14] M. Hintermüller and K. Kunisch. Total bounded variation regularization as a bilaterally constrained optimization problem. *SIAM Journal on Applied Mathematics*, 64(4):1311–1333, 2004.
 - [15] M. Hintermüller and A. Langer. Subspace correction methods for a class of nonsmooth and nonadditive convex variational problems with mixed L^1/L^2 data-fidelity in image processing. *SIAM J. Imaging Sci.*, 6(4):2134–2173, 2013.
 - [16] M. Hintermüller and A. Langer. Surrogate functional based subspace correction methods for image processing. In *Domain Decomposition Methods in Science and Engineering XXI*, pages 829–837. Springer, Cham, 2014.
 - [17] M. Hintermüller and A. Langer. Non-overlapping domain decomposition methods for dual total variation based image denoising. *Journal of Scientific Computing*, 62(2):456–481, 2015.
 - [18] K. Ito and K. Kunisch. *Lagrange Multiplier Approach to Variational Problems and Applications*. Advances in Design and Control. SIAM, Philadelphia, 2008.
 - [19] A. Langer. Domain decomposition for non-smooth (in particular TV) minimization. In *Handbook of Mathematical Models and Algorithms in Computer Vision and Imaging: Mathematical Imaging and Vision*, pages 1–47. Springer, Cham, 2021.
 - [20] A. Langer and F. Gaspoz. Overlapping domain decomposition methods for total variation denoising. *SIAM Journal on Numerical Analysis*, 57(3):1411–1444, 2019.
 - [21] A. Langer, S. Osher, and C.-B. Schönlieb. Bregmanized domain decomposition for image restoration. *Journal of Scientific Computing*, 54(2-3):549–576, 2013.
 - [22] C.-O. Lee and C. Nam. Primal domain decomposition methods for the total variation minimization, based on dual decomposition. *SIAM Journal on Scientific Computing*, 39(2):B403–B423, 2017.
 - [23] C.-O. Lee, C. Nam, and J. Park. Domain decomposition methods using dual conversion for the total variation minimization with L^1 fidelity term. *Journal of Scientific Computing*, 78(2):951–970, 2019.
 - [24] C.-O. Lee, E.-H. Park, and J. Park. A finite element approach for the dual Rudin–Osher–Fatemi model and its nonoverlapping domain decomposition methods. *SIAM Journal on Scientific Computing*, 41(2):B205–B228, 2019.
 - [25] C.-O. Lee and J. Park. Fast nonoverlapping block Jacobi method for the dual Rudin–Osher–Fatemi model. *SIAM Journal on Imaging Sciences*, 12(4):2009–2034, 2019.
 - [26] C.-O. Lee and J. Park. A finite element nonoverlapping domain decomposition method with Lagrange multipliers for the dual total variation minimizations. *Journal of Scientific Computing*, 81(3):2331–2355, 2019.

- [27] C.-O. Lee and J. Park. Recent advances in domain decomposition methods for total variation minimization. *Journal of the Korean Society for Industrial and Applied Mathematics*, 24(2):161–197, 2020.
- [28] X. Li, Z. Zhang, H. Chang, and Y. Duan. Accelerated non-overlapping domain decomposition method for total variation minimization. *Numerical Mathematics: Theory, Methods & Applications*, 14(4), 2021.
- [29] J. Mairal. Optimization with first-order surrogate functions. In *International Conference on Machine Learning*, pages 783–791, 2013.
- [30] J. Park. Additive Schwarz methods for convex optimization as gradient methods. *SIAM Journal on Numerical Analysis*, 58(3):1495–1530, 2020.
- [31] J. Park. An overlapping domain decomposition framework without dual formulation for variational imaging problems. *Advances in Computational Mathematics*, 46(4):1–29, 2020.
- [32] J. Park. Accelerated additive Schwarz methods for convex optimization with adaptive restart. *Journal of Scientific Computing*, 89(3):1–20, 2021.
- [33] A. Quarteroni and A. Valli. *Domain decomposition methods for partial differential equations*. Clarendon Press, Oxford, 1999.
- [34] A. Toselli and O. B. Widlund. *Domain decomposition methods: algorithms and theory*, volume 34. Springer, Berlin, Heidelberg, 2005.